Applied Mathematics & Information Sciences
An International Journal

http://dx.doi.org/10.18576/amis/200617

Theory and Finite-Sample Inference for a Novel Circular Probability Distribution in Directional Statistics

Mohamed S. Eliwa[1], *Hend S. Shahen*[2,*], *and Mahmoud El-Morshedy*[2]

[1]Department of Mathematics, Faculty of Science, Mansoura University, Mansoura 35516, Egypt
[2]Department of Mathematics, College of Science and Humanities in Al-Kharj, Prince Sattam bin Abdulaziz University, Al-Kharj 11942, Saudi Arabia

Received: 12 Sep. 2026, Revised: 20 Oct. 2026, Accepted: 27 Oct. 2026
Published online: 1 Nov. 2026

Abstract: In this paper, we offer a new circular probability model with a single parameter by translating a one-parameter linear-exponential distribution on a circle of $[0, 2\pi)$. The resulting model, referred to as the wrapped one-parameter linear-exponential (WrOPLE) distribution, has closed form expressions for both probability density and cumulative distribution functions, which enable an analytically tractable examination of crucial probabilistic and directional features. Explicit formulas are derived for the wrapped and unwrapped characteristic functions, trigonometric moments, mean direction, mean resultant length, circular variance, circular standard deviation and measurements of circular skewness and kurtosis. The features of reliability theory are explored, including the hazard rate function, reversed hazard rate function, mean residual life and mean inactivity time and their boundary properties. We explore the geometrical and asymptotic aspects of the model by means of the density-shape, the limiting behavior and modality. There are well known requirements for the shift of the density from an internal unimodal configuration to a boundary mode. In this study, the method of maximum likelihood estimation of the unknown parameter is established and a Monte Carlo simulation analysis of the finite sample performance is undertaken for different parameter settings and sizes of the sample exhibiting greater estimate accuracy in larger sample size. We evaluate our methods on real directed data sets and compare to known wrapped distributions via probability based metrics, circular summary statistics and visual examination. The WrOPLE distribution provides a flexible and analytically tractable extension of the wrapped model family for the directional sustainability data considered, delivering competitive performance within a parsimonious one-parameter framework.

Keywords: Directional statistics; Circular probability distributions; Trigonometric moments; Failure analysis; Parameter estimation; Goodness-of-fit; Monte Carlo simulation

1 Introduction

Circular data is when the measured result is a direction, orientation, bearing, or phase rather than a linear measurement. Typical examples encountered in sustainability research include wind direction in meteorology, animal migration trajectories in ecology, fracture or fault orientations in geology, paleomagnetic declinations in geophysics, and rhythmic phase assessments in biology and medicine (e.g., circadian activity patterns). The similarities between these contexts are that angular quantities are periodic: the same physical direction is represented by values that are separated by an integer multiple of 2π. So the natural sample space is the unit circle S^1, and the operational meanings of "distance", "location", and "spread" are profoundly transformed by its non-Euclidean topology and geometry. Classical texts [1], [2], [3] provide comprehensive reviews of these basic topics and their statistical implications. The cyclic nature of S^1 means that one should not directly use linear summaries and inferential techniques, as they are not only insufficient but may also be misleading. For example, linear averaging fails near the branch cut (e.g. 1° and 359° give an average of 180°), leading in estimates inconsistent with the fundamental geometry. Similarly, linear measures of spread treat 0 and 2π as far apart, while they are equivalent on the circle. These requirements require essentially circular metrics like mean direction and circular variance which are more suitably expressed in terms of trigonometric moments and

* Corresponding author e-mail: h.shahen@psau.edu.sa

© 2026 NSP
Natural Sciences Publishing Cor.

resultant length rather than conventional moments; see, for example, [1, 2, 3]. Likelihood based estimation, regression and hypothesis testing need the existence of probability models on $[0,2\pi)$ (or $(-\pi,\pi]$) that are periodic and have parameters with a meaningful direction from an inferential point of view.

There are several circular distributions including the von Mises, cardioid, wrapped normal and wrapped Cauchy families [1, 2]. Modern applications are increasingly exhibiting features that break classic models: asymmetry arising from environmental constraints, multimodality arising from various subpopulations, and heavy-tailed angular behavior due to sporadic dynamics or measurement methodologies. Symmetry about a singular mean direction is sometimes empirically doubtful; under symmetric frameworks (e.g., von Mises) this can lead to biased location estimate, mischaracterized uncertainty assessment, and inadequate tail fitting. These concerns have led to the continual development of asymmetric and skewed circular distributions and their empirical validation on real research [4, 5, 6].

One popular and well-regarded approach for generating circular distributions is wrapping: A linear random variable is reduced modulo 2π on S^1. Wrapping familiar real line models into a circular framework often preserves the interpretability of the parent parameters and allows for the systematic transfer of distributional features (e.g., skewness, tail behavior) to the circular domain [1, 3]. Formally, if X is a nonnegative random variable with probability density function (PDF) $f(x)$ on $(0,\infty)$, then the circular PDF of

$$\Theta = X \bmod 2\pi$$

is

$$g(\theta) = \sum_{k=0}^{\infty} f(\theta + 2\pi k), \qquad 0 \le \theta < 2\pi. \tag{1}$$

The equation in (1) can be understood as a "method of images": the probability mass on the line is constantly folded onto the interval $[0,2\pi)$. The design guaranties periodicity, $g(\theta) = g(\theta + 2\pi)$, and it is able to describe sophisticated asymmetric behavior when the parent density is biased.

Recent research have suggested that lifetime (survival) distributions are attractive as basic models for wrapping. These families are naturally defined on $(0,\infty)$ and display recognizable shape features (e.g., increasing/decreasing failure rates) and a large range of skewness and tail weight given a parsimonious parameterization. These qualities often create practically useful asymmetric circular densities for directed data which show large deviations from symmetry when wrapped. Thus, some wrapped lifetime models have been presented, for example wrapped Lindley-type and related models, wrapped weighted exponential models and other wrapped families to enhance skewness and flexibility in [8, 9, 10, 11, 12, 13, 14], and [17, 18, 19]. The study of circular data and its applications can be found in [15, 16, 20]. These contributions together show that nicely skewed linear parents can create circular laws better than the classical symmetric ones in many applications. At the same time, wrapping presents lasting methodological limits that are not merely technical irritants but can seriously hamper inference. The definition (1) usually provides probability density functions and cumulative distribution functions only in the form of infinite series at first. This, however, necessitates truncation, which (i) incurs approximation errors that may be large in the tails or in the case of weak concentration, (ii) complicates maximum likelihood estimation, as gradients and Hessians must also be approximated by series, and (iii) obfuscates analytic expressions for trigonometric moments and related circular measures. Second, wrapping can produce likelihood surfaces that are numerically unstable for high concentrations or small sample sizes, which is common in directional research (e.g., specialized geological assessments or animal tracking with few subjects). Thirdly, more flexible models with more parameters may worsen the problems of identifiability and convergence, especially when the circular sample provides little information about higher-order shape features. These considerations motivate the search for parsimonious circular models that are sufficiently flexible to allow for asymmetry and heterogeneity, yet nevertheless allow for accurate moment calculations and efficient likelihood-based inference.

We offer a new asymmetric circular model motivated by this need, by wrapping the one-parameter linear-exponential (LE) distribution introduced by Sah [7]. The LE family is a simple extension of the exponential law, where the exponential kernel is multiplied by a linear polynomial. This results in an improved flexibility in shape, while preserving the analytical simplicity. Enveloping this parent distribution on S^1 yields the wrapped one-parameter linear exponential (WrOPLE) distribution. An important aspect of this framework is that, contrary to many wrapped lifetime models whose densities are expressed as infinite series, the summation in (1) can be calculated in closed form, yielding closed-form expressions for the PDF and the cumulative distribution function (CDF). This convenience enables for accurate computation of trigonometric moments and common circular statistics (mean direction, resultant length, circular variance, skewness), as well as maximum likelihood estimation free of truncation error, and efficient random number generation.

The remainder of this paper is organized as follows. Section 2 proposes a WrOPLE distribution and provides exact closed-form expressions for its probability density function (PDF) and cumulative distribution function (CDF), with graphical illustrations in both linear (real-line) and circular plots on S^1. The main analytic properties of the model are described in Section 3. These include limiting behavior and derivative properties, modal

© 2026 NSP
Natural Sciences Publishing Cor.

behavior and associated shape properties, the relationship between the characteristic functions of the wrapped and unwrapped forms, and closed form trigonometric moments and conventional measures of circular location and spread. Also, several aspects of the functions of the hazard rate, the reversed hazard rate, the mean residual life and the mean inactivity time are explored for the characteristics of the reliability theory. Section 4 describes maximum likelihood estimation of parameters, and assesses numerical efficiency on simulated data, with the effect of truncation and approximation decisions where relevant. An detailed simulation study is presented in Section 5 to assess the finite-sample performance of the proposed inferential procedures. In Section 6, we assess the real-world relevance of the WrOPLE model by fitting it to sustainability directional datasets and contrasting its performance with that of established circular competitors. Section 7 concludes with analysis of data and defines possible extensions.

2 The Wrapped OPLE Distribution: Theoretical Development and Linear/Circular Views

In this segment, we delineate the suggested circular model derived by encircling the one-parameter linear exponential (OPLE) distribution of Sah [7] around the unit circle. Let X be a nonnegative stochastic variable that adheres to the OPLE model with a parameter $\beta > 0$. The PDF is as follows.

$$f(x;\beta) = \frac{\beta^2}{1+\beta^3}(\beta^2+x)e^{-\beta x}, \qquad x>0,\ \beta>0, \quad (2)$$

and the corresponding CDF is

$$F(x;\beta) = 1 - \frac{1+\beta x+\beta^3}{1+\beta^3}e^{-\beta x}, \qquad x>0,\ \beta>0. \quad (3)$$

Define the wrapped random variable

$$\Theta = X \pmod{2\pi}, \qquad 0 \le \Theta < 2\pi, \quad (4)$$

so that Θ represents the angle obtained by reducing X modulo 2π. The PDF of the WrOPLE distribution is given by the standard wrapping formula

$$g(\theta;\beta) = \sum_{k=0}^{\infty} f(\theta+2\pi k;\beta), \qquad 0 \le \theta < 2\pi,\ \beta>0. \quad (5)$$

Substituting (2) into (5) and Assessing the resultant geometric series produces the subsequent closed expression for the WrOPLE density:

$$\begin{aligned} g(\theta;\beta) = {} & \frac{\beta^2 e^{2\beta\pi}}{(1+\beta^3)e^{\beta\theta}(e^{2\beta\pi}-1)^2} \\ & \times \Big[(\beta^2+\theta)e^{2\beta\pi} \\ & -\beta^2-\theta+2\pi\Big], \\ & 0 \le \theta < 2\pi, \quad \beta>0. \end{aligned} \quad (6)$$

The asymptotic characteristics of the PDF of the WrOPLE model at the edges of the support $[0,2\pi)$ demonstrate significant continuity attributes. As θ nears the lower limit 0^+, we derive:

$$\begin{aligned} \lim_{\theta\to 0^+} g(\theta;\beta) = {} & \frac{\beta^2 e^{2\beta\pi}}{(1+\beta^3)(e^{2\beta\pi}-1)^2} \\ & \times \Big[\beta^2(e^{2\beta\pi}-1)+2\pi\Big]. \end{aligned} \quad (7)$$

while at the upper boundary $2\pi^-$, the limit is given by:

$$\begin{aligned} \lim_{\theta\to 2\pi^-} g(\theta;\beta) = {} & \frac{\beta^2 e^{2\beta\pi}}{(1+\beta^3)e^{2\pi\beta}(e^{2\beta\pi}-1)^2} \\ & \times \Big[(\beta^2+2\pi)e^{2\beta\pi}-\beta^2\Big]. \end{aligned} \quad (8)$$

These restrictions show that for all positive values of β the boundary behavior of the PDF is well defined, thus encircling the circle properly. The fact that these two limits are equal ensures the continuity of the wrapped distribution, which is a necessary condition for a valid circular probability model. The wrapped CDF can be written as

$$\begin{aligned} G(\theta;\beta) = {} & \sum_{k=0}^{\infty}\Big[F(\theta+2\pi k;\beta) \\ & -F(2\pi k;\beta)\Big], \\ & 0 \le \theta < 2\pi,\ \beta>0, \end{aligned} \quad (9)$$

which simplifies to the explicit closed form

$$\begin{aligned} G(\theta;\beta) = {} & \frac{1}{(1+\beta^3)(e^{2\beta\pi}-1)^2}\Big[(1+\beta^3)e^{4\beta\pi} \\ & -(\beta^3-2\beta\pi+1)e^{2\beta\pi} \\ & -(1+\beta\theta+\beta^3)e^{\beta(-\theta+4\pi)} \\ & +(1+\beta\theta-2\beta\pi+\beta^3)e^{\beta(-\theta+2\pi)}\Big], \end{aligned} \quad (10)$$

where $0 \le \theta < 2\pi$ and $\beta > 0$. The WrOPLE distribution is a circular model characterized by a single parameter, with a closed-form PDF and CDF, hence eliminating the necessity for series truncation in likelihood assessment and facilitating precise computation of trigonometric moments. Figures 1 and 2 illustrate the effect of the parameter β on the arrangement of the proposed model. When β increases, the probability density becomes more concentrated around the origin, a trait that is also apparent in the increase of the mean resultant length presented in Table 1.

© 2026 NSP
Natural Sciences Publishing Cor.

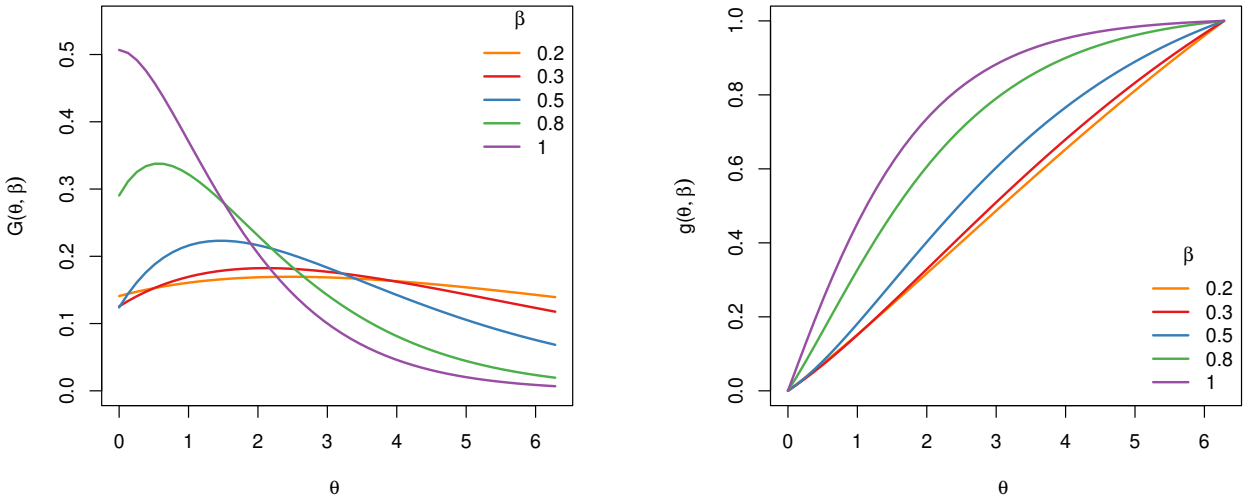


Fig. 1: Linear-scale plots of the WrOPLE distribution: PDF (left panel) and CDF (right panel).

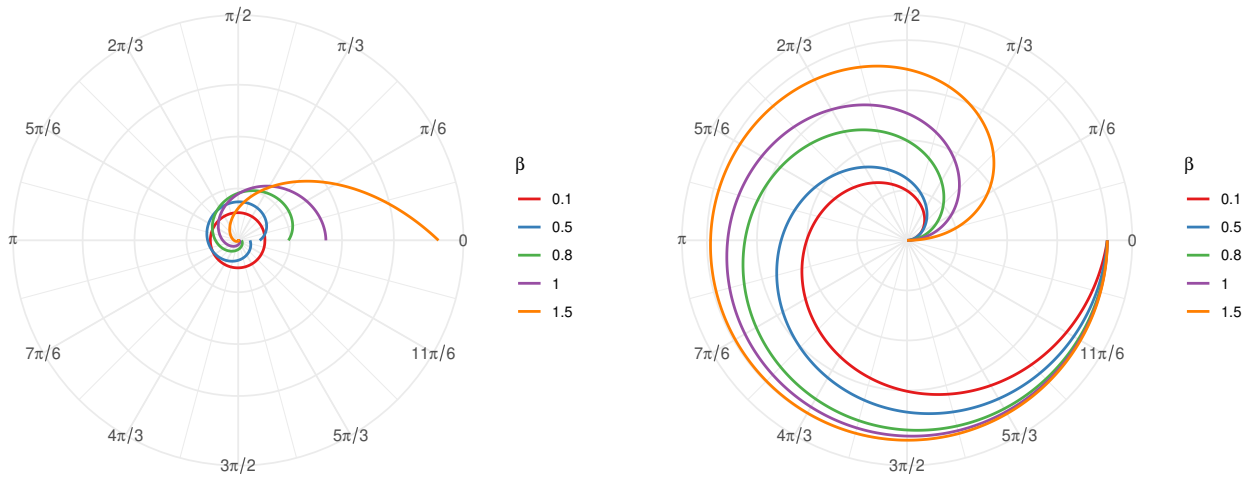


Fig. 2: Circular representations of the WrOPLE distribution: PDF (left panel) and CDF (right panel).

3 Metric Distributions and Properties

3.1 Morphological Transitions: From Unimodal Profiles to Boundary Localization

The modal configuration of the WrOPLE distribution shows interesting variations depending on the shape parameter β. In this section, we provide a detailed analysis of this behavior. Critical points of the density function are obtained by solving $g'(\theta;\beta) = 0$. Hence,

$$\theta_0 = \frac{-(1-\beta^3)(1-e^{2\pi\beta}) - 2\pi\beta}{\beta(e^{2\pi\beta}-1)}. \qquad (11)$$

To see whether θ_0 is a local maximum (rather than a minimum or point of inflection) we compute the second derivative at this critical point. For $\theta_0 \in (0, 2\pi)$ we have

© 2026 NSP
Natural Sciences Publishing Cor.

that

$$g''(\theta_0;\beta) = \frac{-\beta^3}{(1+\beta^3)(e^{2\pi\beta}-1)} \times \exp\left\{ \frac{(2\pi\beta+\beta^3-1)e^{2\pi\beta}}{e^{2\pi\beta}-1} - \frac{\beta^3-1}{e^{2\pi\beta}-1} \right\} < 0, \tag{12}$$

verifying that θ_0 constitutes a local maximum whenever it resides within the support. A fundamental element of the modal behavior of the WrOPLE distribution is the parameter-dependent shift between interior and boundary modes. The candidate mode θ_0 from (11) is deemed positive (and therefore a legitimate interior mode) solely under the following condition:

$$(1-\beta^3)(e^{2\pi\beta}-1) - 2\pi\beta > 0. \tag{13}$$

The equality in (13) defines a crucial threshold value β_0 which can be determined mathematically. The solution of this transcendental equation gives:

$$\beta_0 \approx 0.99598. \tag{14}$$

This critical value partitions the parameter space into two distinct regimes:

- **–Unimodal regime** ($0 < \beta < \beta_0$): The density has an interior mode at θ_0 given by (11).
- **–Boundary mode regime** ($\beta \geq \beta_0$): The interior candidate falls outside $(0, 2\pi)$, and the maximum occurs at the boundary $\theta = 0$.

This transition is a vital change in the shape characteristics of the distribution and has important implications for data modeling and analysis. For concentrated circular data, i.e., for small values of $1-\beta$, values of β close to or larger than β_0 may be particularly appropriate.

3.2 Spectral Duality Between Periodic and Aperiodic Characteristic Functions

The characteristic function completely characterizes a probability distribution. It is frequently used to determine moments and to investigate properties of distributions. The key result of [15] is that the pth order trigonometric moments of a wrapped circular distribution, $\phi^*_\theta(p)$, are equal to the characteristic function of the unwrapped random variable X, $\phi_X(t)$, evaluated at integer points $t = p$.

$$\phi^*_\theta(p) = \phi_X(p), \quad p \in \mathbb{Z}. \tag{15}$$

This wrapping property greatly simplifies the computation of circular moments. The characteristic function for the basic OPLE distribution is:

$$\phi_X(t) = \mathbb{E}\left(e^{itX}\right) = \frac{\beta^2}{1+\beta^3}(\beta - it)^{-2} \times (1+\beta^3 - it\beta^2), \quad t \in \mathbb{R}, \tag{16}$$

where $i = \sqrt{-1}$ denotes the imaginary unit. According to the wrapping property (15), the characteristic function of the WrOPLE distribution is derived by assessing (16) at integer points:

$$\phi^*_\theta(p) = \mathbb{E}(e^{i\theta p}) = \frac{\beta^2}{1+\beta^3}(\beta - ip)^{-2} \times (1+\beta^3 - ip\beta^2), \quad p \in \mathbb{Z}\setminus\{0\}, \tag{17}$$

To find the characteristic function in the polar form (magnitude and angle) we use the De Moivre's theorem. For any complex number $(a-ib)^{-n}$ where $a, b, n \in \mathbb{R}$ we can write.

$$(a-ib)^{-n} = \left(\sqrt{a^2+b^2}\right)^{-n} e^{in\arctan(b/a)}. \tag{18}$$

Applying this to the terms in (17):

$$(\beta - ip)^{-2} = \frac{1}{\beta^2+p^2} \times \exp\left\{2i\arctan\left(\frac{p}{\beta}\right)\right\}, \tag{19}$$

$$(1+\beta^3 - ip\beta^2) = \sqrt{(1+\beta^3)^2 + p^2\beta^4} \times \exp\left\{-i\arctan\left(\frac{p\beta^2}{1+\beta^3}\right)\right\}. \tag{20}$$

Substituting (19) and (20) into (17), the characteristic function becomes:

$$\phi^*_\theta(p) = \frac{\beta^2\sqrt{(1+\beta^3)^2+p^2\beta^4}}{(1+\beta^3)(\beta^2+p^2)} \times \exp\left\{ i\left[2\arctan\left(\frac{p}{\beta}\right) - \arctan\left(\frac{p\beta^2}{1+\beta^3}\right)\right]\right\}, \tag{21}$$

This polar representation enables the derivation of trigonometric moments, as elaborated in the subsequent subsection.

3.3 Circular Distributional Properties: Trigonometric Moments

Trigonometric moments are circular analogs of classical moments and provide basic descriptive measures for

© 2026 NSP
Natural Sciences Publishing Cor.

circular distributions. Following the convention in directional statistics [15], any trigonometric moment can be stated in polar coordinates as:

$$\phi_\theta^*(p) = \rho_p e^{i\mu_p}, \tag{22}$$

where $\rho_p \in [0,1]$ is the pth-order mean resultant length, and $\mu_p \in [0, 2\pi)$ is the pth-order mean direction. Comparing (21) with the conventional polar representation (22) we immediately obtain:

$$\rho_p = \frac{\beta^2\sqrt{(1+\beta^3)^2+p^2\beta^4}}{(1+\beta^3)(\beta^2+p^2)}, \tag{23}$$

and

$$\mu_p = 2\arctan\left(\frac{p}{\beta}\right) - \arctan\left(\frac{p\beta^2}{1+\beta^3}\right). \tag{24}$$

The most commonly used circular descriptive statistics are those based on the first-order trigonometric moment ($p = 1$). The circular mean direction is defined by:

$$\mu = \mu_1 = 2\arctan\left(\frac{1}{\beta}\right) - \arctan\left(\frac{\beta^2}{1+\beta^3}\right). \tag{25}$$

It is the mean angular orientation of the distribution. In the WrOPLE distribution, μ is a decreasing function of β, with $\mu \sim \pi$ as $\beta \to 0$ and $\mu \to 0$ as $\beta \to \infty$. The average length (or concentration parameter) resulting is:

$$\rho = \rho_1 = \frac{\beta^2\sqrt{(1+\beta^3)^2+\beta^4}}{(1+\beta^3)(\beta^2+1)}. \tag{26}$$

This quantity measures the density of the distribution relative to the mean direction. $\rho = 0$ means that the data is uniformly dispersed and $\rho = 1$ that the data is concentrated. Circular variance gives a measure of dispersion:

$$V_0 = 1 - \rho_1 = 1 - \frac{\beta^2\sqrt{(1+\beta^3)^2+\beta^4}}{(1+\beta^3)(\beta^2+1)}. \tag{27}$$

Unlike linear variance, circular variance ranges between 0 (perfect concentration) and 1 (uniform dispersion). The circular standard deviation is defined as:

$$\begin{aligned}\sigma_0 &= \sqrt{-2\ln(1-V_0)} \\ &= \sqrt{-2\ln\left(\frac{\beta^2\sqrt{(1+\beta^3)^2+\beta^4}}{(1+\beta^3)(\beta^2+1)}\right)},\end{aligned} \tag{28}$$

This metric provides a measure of angular dispersion and is particularly useful in delineation of confidence regions. In contrast, the pth trigonometric moment can be expressed in Cartesian coordinates as:

$$\phi_\theta^*(p) = \alpha_p + i\beta_p, \tag{29}$$

where the real and imaginary components are given by:

$$\begin{aligned}\alpha_p &= \rho_p\cos(\mu_p) \\ &= \frac{\beta^2\sqrt{(1+\beta^3)^2+p^2\beta^4}}{(1+\beta^3)(\beta^2+p^2)} \\ &\quad\times\cos\left[2\arctan\left(\frac{p}{\beta}\right)\right. \\ &\quad\left.-\arctan\left(\frac{p\beta^2}{1+\beta^3}\right)\right],\end{aligned} \tag{30}$$

and

$$\begin{aligned}\beta_p &= \rho_p\sin(\mu_p) \\ &= \frac{\beta^2\sqrt{(1+\beta^3)^2+p^2\beta^4}}{(1+\beta^3)(\beta^2+p^2)} \\ &\quad\times\sin\left[2\arctan\left(\frac{p}{\beta}\right)\right. \\ &\quad\left.-\arctan\left(\frac{p\beta^2}{1+\beta^3}\right)\right],\end{aligned} \tag{31}$$

These Cartesian elements are very advantageous for testing hypotheses and visual representation. Central trigonometric moments are derived by centering on the mean direction μ_1, similar to central moments in linear statistics.

$$\overline{\alpha}_p = \rho_p\cos(\mu_p - p\mu_1), \tag{32}$$

and

$$\overline{\beta}_p = \rho_p\sin(\mu_p - p\mu_1). \tag{33}$$

For the WrOPLE distribution, they transform into:

$$\overline{\alpha}_p = \frac{\beta^2\sqrt{(1+\beta^3)^2+p^2\beta^4}}{(1+\beta^3)(\beta^2+p^2)}\cos(\Psi_{p,\beta}), \tag{34}$$

and

$$\overline{\beta}_p = \frac{\beta^2\sqrt{(1+\beta^3)^2+p^2\beta^4}}{(1+\beta^3)(\beta^2+p^2)}\sin(\Psi_{p,\beta}), \tag{35}$$

where the centering angle is defined as:

$$\begin{aligned}\Psi_{p,\beta} &= 2\left[\arctan\left(\frac{p}{\beta}\right) - p\arctan\left(\frac{1}{\beta}\right)\right] \\ &\quad-\arctan\left(\frac{p\beta^2}{1+\beta^3}\right) \\ &\quad+p\arctan\left(\frac{\beta^2}{1+\beta^3}\right).\end{aligned} \tag{36}$$

Note that by construction $\overline{\beta}_1 = 0$, which implies that the first central moment has no imaginary part. Higher order shape qualities can be described by use of central trigonometric moments. The circular skewness parameter

© 2026 NSP
Natural Sciences Publishing Cor.

is:

$$\begin{aligned}\phi_1^0 &= \frac{\overline{\beta}_2}{V_0^{3/2}} \\ &= \frac{\beta^2\sqrt{(1+\beta^3)^2+4\beta^4}}{(1+\beta^3)(\beta^2+4)} \\ &\times \left[1-\frac{\beta^2\sqrt{(1+\beta^3)^2+\beta^4}}{(1+\beta^3)(\beta^2+1)}\right]^{-3/2} \\ &\times \sin(\Psi_{2,\beta}),\end{aligned} \tag{37}$$

The metric measures the asymmetry of the distribution around its mean direction. When the circular kurtosis coefficient is defined as:

$$\phi_2^0 = \frac{\overline{\alpha}_2-(1-V_0)^4}{V_0^2}, \tag{38}$$

which, upon substitution, becomes:

$$\begin{aligned}\phi_2^0 &= \left[\frac{\beta^2\sqrt{(1+\beta^3)^2+4\beta^4}}{(1+\beta^3)(\beta^2+4)}\right. \\ &\times \cos(\Psi_{2,\beta}) - \left.\left(\frac{\beta^2\sqrt{(1+\beta^3)^2+\beta^4}}{(1+\beta^3)(\beta^2+1)}\right)^4\right] \\ &\times \left[1-\frac{\beta^2\sqrt{(1+\beta^3)^2+\beta^4}}{(1+\beta^3)(\beta^2+1)}\right]^{-2},\end{aligned} \tag{39}$$

where

$$\begin{aligned}\Psi_{2,\beta} &= 2\left[\arctan\left(\frac{2}{\beta}\right) - 2\arctan\left(\frac{1}{\beta}\right)\right] \\ &- \arctan\left(\frac{2\beta^2}{1+\beta^3}\right) \\ &+ 2\arctan\left(\frac{\beta^2}{1+\beta^3}\right).\end{aligned} \tag{40}$$

This metric describes the shape of the distribution, i.e. its peakedness and tails. Table 1 gives a complete numerical summary of the circular properties of the WrOPLE distribution for various values of the shape parameter. The table illustrates the transition from a mostly uniform, random distribution at low β values to a highly concentrated, peaked distribution at high β values.

As β increases from 0.1 to 3.0, the results in Table 1 demonstrate several important distributional patterns. The mean resultant length ρ shows a continuous increase from close to zero to close to one, showing a transition from high dispersion to high concentration. Meanwhile, the mean direction μ decreases from about 2.93 rad (about π) to 0.33 rad (approximately 0), in agreement with the boundary mode properties. For form, the circular skewness ϕ_1^0 slowly goes negative, indicating an increase in asymmetry with a long tail in the positive angular direction. Also, the distribution changes from a platykurtic form at lower β values to a substantially leptokurtic form at higher values. The central trigonometric moments $\overline{\alpha}_p$ and $\overline{\beta}_p$ offer more support for these patterns of concentration and asymmetry. All these features show the flexibility of WrOPLE distribution to model a wide variety of circular data, from almost uniform to highly concentrated ones.

3.4 Reliability Analysis

In this section we define the basic reliability functions of the WrOPLE distribution. We employ the PDF $g(\theta;\beta)$ as in (6) and the CDF $G(\theta;\beta)$ as in (10). To be brief, let us say that the common normalizing denominator is $\mathscr{D} = (1+\beta^3)(e^{2\beta\pi}-1)^2$.

3.4.1 Reversed (Hazard) Rate Function: Analytical Behavior and Limits

The hazard rate function (HRF), $h(\theta;\beta)$, is the instantaneous failure rate at time θ given survival to time θ. It is quantitatively defined as a ratio between the PDF and the survival function. $S(\theta;\beta) = 1-G(\theta;\beta)$:

$$h(\theta;\beta) = \frac{g(\theta;\beta)}{1-G(\theta;\beta)},\ 0 \le \theta < 2\pi. \tag{41}$$

Substituting the explicit forms of $g(\theta;\beta)$ and $G(\theta;\beta)$ leads to a difficult rational-exponential function, so we examine its boundary properties. When $\theta \to 0^+$, then $G(0;\beta) = 0$, so that $S(0;\beta) = 1$, i.e., the initial HRF coincides with the initial density.

$$h(0;\beta) = g(0;\beta) = \frac{\beta^2 e^{2\beta\pi}\left[(\beta^2)(e^{2\beta\pi}-1)+2\pi\right]}{\mathscr{D}}.$$

In contrast, as $\theta \to 2\pi^-$, we have $G(2\pi;\beta) = 1$, so that $S(\theta;\beta) \to 0$, while the density at the upper limit remains finite and non-zero.

$$\begin{aligned}g(2\pi;\beta) &= \frac{\beta^2 e^{2\beta\pi}}{(1+\beta^3)e^{2\beta\pi}(e^{2\beta\pi}-1)^2} \\ &\times \left[(\beta^2+2\pi)(e^{2\beta\pi}-1)+2\pi\right] > 0.\end{aligned}$$

Therefore, the HRF has a singularity at the upper bound,

$$\lim_{\theta\to 2\pi^-} h(\theta;\beta) = +\infty,$$

which shows an increasing failure rate (IFR) pattern around 2π, as is typical of distributions with bounded support. The HRF is shown in Figure 3. Thus, an HRF produces a linear progression from a given angular point and its meaning for circular data is of a basic dependence on that point. This is a mathematical property from the wrapped CDF across the defined interval $[0,2\pi)$ as proven. The reversed HRF (RHRF), $\tau(\theta;\beta)$, is an

© 2026 NSP
Natural Sciences Publishing Cor.

Table 1: Circular properties of the WrOPLE distribution for specific values of the shape parameter β.

Characteristic		Shape parameter β							
Category	**Notation**	0.1	0.3	0.5	0.7	0.9	1.0	1.5	3.0
Primary location and dispersion measures									
Mean direction	μ (rad)	2.9323	2.4713	1.9956	1.5703	1.2378	1.1071	0.7010	0.3325
Resultant length	ρ	0.0099	0.0829	0.2049	0.3501	0.4942	0.5590	0.7785	0.9453
Circular variance	V_0	0.9901	0.9171	0.7951	0.6499	0.5058	0.4410	0.2215	0.0547
Circular std. dev.	σ_0 (rad)	3.0381	2.2317	1.7806	1.4489	1.1873	1.0785	0.7077	0.3353
Shape characteristics									
Circular skewness	ϕ_1^0	−0.0007	−0.0194	−0.0892	−0.2486	−0.5153	−0.6830	−1.6842	−3.8846
Circular kurtosis	ϕ_2^0	−0.0024	−0.0172	−0.0217	0.0492	0.3042	0.5263	2.4127	7.6502
Non-central trigonometric moments (Cartesian form)									
First cosine	α_1	−0.0097	−0.0650	−0.0844	0.0002	0.1615	0.2500	0.5949	0.8936
Second cosine	α_2	−0.0025	−0.0199	−0.0396	−0.0357	0.0064	0.0400	0.2547	0.6771
First sine	β_1	0.0021	0.0515	0.1867	0.3501	0.4670	0.5000	0.5021	0.3086
Second sine	β_2	0.0003	0.0101	0.0507	0.1303	0.2307	0.2800	0.4493	0.4679
Central trigonometric moments (Cartesian form)									
First cosine	$\overline{\alpha}_1$	0.0099	0.0829	0.2049	0.3501	0.4942	0.5590	0.7785	0.9453
Second cosine	$\overline{\alpha}_2$	−0.0024	−0.0144	−0.0120	0.0358	0.1375	0.2000	0.4857	0.8215
First sine	$\overline{\beta}_1$	0	0	0	0	0	0	0	0
Second sine	$\overline{\beta}_2$	−0.0007	−0.0171	−0.0632	−0.1303	−0.1854	−0.2000	−0.1756	−0.0496

important quantity in the analysis of left-censored data, and is given by:

$$\tau(\theta;\beta) = \frac{g(\theta;\beta)}{G(\theta;\beta)}, \qquad 0 < \theta \leq 2\pi. \tag{42}$$

The RHRF has a number of important properties. First of all, it has a singularity at the origin: since $G(0;\beta) = 0$ and $g(0;\beta) > 0$, by L'Hopital's approach (or just evaluating the limit) we get

$$\lim_{\theta \to 0^+} \tau(\theta;\beta) = +\infty.$$

Secondly, it is finite at the end point, $\theta = 2\pi$, since $G(2\pi;\beta) = 1$, the RHRF becomes the PDF value at the boundary and as such $\tau(2\pi;\beta) = g(2\pi;\beta) < \infty$. Finally, in terms of monotonicity, the RHRF is strictly decreasing when the base density is log-concave around zero, which is the case in general for the exponential polynomial form of the WrOPLE model over usual ranges of the parameters.

3.4.2 Mean Residual Life Function

The mean residual life (MRL) function, $m(\theta;\beta)$, is the expected remaining life (angle) assuming that the individual survives to time θ. It is described by the ratio of the integral of the survival function to the likelihood of survival:

$$m(\theta;\beta) = E[\Theta - \theta \mid \Theta > \theta] = \frac{\int_\theta^{2\pi} S(u;\beta)\,du}{S(\theta;\beta)}. \tag{43}$$

To get the explicit mathematical expression we compute the numerator. $m_N(\theta) = \int_\theta^{2\pi} S(u)du = [u - \int G(u)du]_\theta^{2\pi}$. Since G(u) consists of terms of the form Ae^{ku} and Bue^{ku}, its integral may be handled analytically. Define $\Psi(\theta)$ as the integral of $G(\theta;\beta)$ in relation to θ. Next up:

$$\begin{aligned}\Psi(\theta) = \frac{1}{\mathscr{D}}\Bigg\{ & \big[(1+\beta^3)e^{4\beta\pi} \\ & -(\beta^3 - 2\beta\pi + 1)e^{2\beta\pi}\big]\theta \\ & -\frac{1+\beta^3}{\beta}e^{\beta(4\pi-\theta)}(1+\beta\theta) \\ & -\frac{1+\beta^3}{\beta^2}e^{\beta(4\pi-\theta)} \\ & +\frac{1+\beta^3-2\beta\pi}{\beta}e^{\beta(2\pi-\theta)}(1+\beta\theta) \\ & +\frac{1+\beta^3-2\beta\pi}{\beta^2}e^{\beta(2\pi-\theta)}\Bigg\}. \end{aligned} \tag{44}$$

© 2026 NSP
Natural Sciences Publishing Cor.

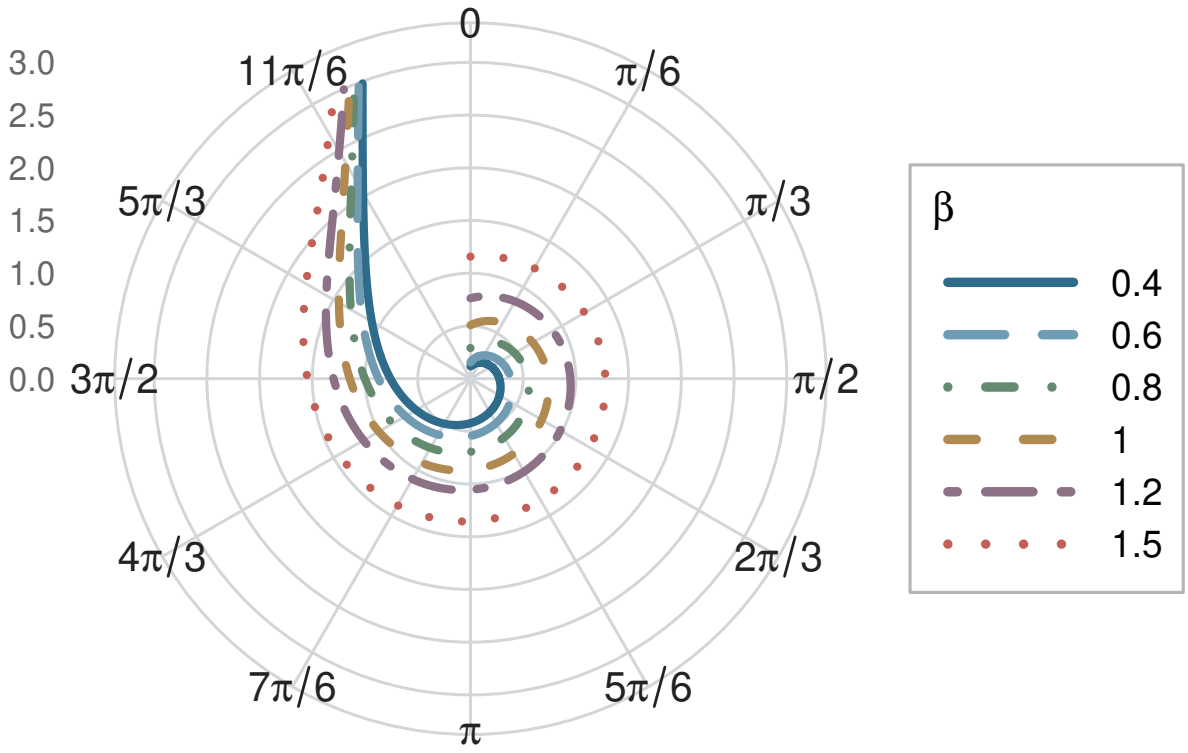


Fig. 3: Circular hazard rate function of the WrOPLE distribution for selected values of the parameter β.

Thus, the exact MRL is:

$$m(\theta;\beta) = \frac{(2\pi-\theta) - \left[\Psi(2\pi) - \Psi(\theta)\right]}{1 - G(\theta;\beta)}. \tag{45}$$

The alteration in the MRL is dictated by the HRF via the essential equation:

$$\frac{d}{d\theta} m(\theta;\beta) = h(\theta;\beta) m(\theta;\beta) - 1. \tag{46}$$

Now, since $h(\theta;\beta) \to \infty$ as $\theta \to 2\pi$, Eq. (46) implies that the gradient of $m(\theta)$ approaches negative infinity at the boundary, which requires that $m(2\pi;\beta) = 0$.

3.4.3 Mean Inactivity Time

Let $r(\theta;\beta)$ be the mean inactivity time (MIT) which measures the expected inactivity time of a failure before θ. It is defined as

$$r(\theta;\beta) = E[\theta - \Theta \mid \Theta \le \theta] = \frac{\int_0^\theta G(u;\beta)\,du}{G(\theta;\beta)}, \quad \theta > 0. \tag{47}$$

The numerator can be evaluated using the antiderivative $\Psi(\theta)$ obtained in Section 3.4.2 as $\int_0^\theta G(u)du = \Psi(\theta) - \Psi(0)$. Hence the exact analytical form of the MIT reads:

$$\begin{aligned} r(\theta;\beta) &= \frac{\Psi(\theta) - \Psi(0)}{G(\theta;\beta)}, \\ \Psi(0) &= -\frac{1}{\mathscr{D}}\left[\frac{K_1}{\beta} e^{4\beta\pi} + \frac{K_1}{\beta^2}\right. \\ &\quad \left. - \frac{K_2}{\beta} e^{2\beta\pi} - \frac{K_2}{\beta^2}\right]. \end{aligned} \tag{48}$$

© 2026 NSP
Natural Sciences Publishing Cor.

where the coefficients of the exponential terms in $G(\theta)$ are $K_1 = 1+\beta^3$ and $K_2 = 1+\beta^3-2\beta\pi$. Like the MRL, the MIT is developed in association with the RHRF.

$$\frac{d}{d\theta} r(\theta;\beta) = \tau(\theta;\beta) r(\theta;\beta) + 1. \tag{49}$$

The boundary conditions are a direct consequence of the properties of $G(\theta)$. When θ tends to 0 from the positive side, we obtain from L'Hôpital's rule on (47)

$$\lim_{\theta\to 0^+} r(\theta) = 0.$$

Furthermore, for the upper limit $\theta = 2\pi$, we obtain

$$r(2\pi;\beta) = \int_0^{2\pi} G(u)\,du = \Psi(2\pi) - \Psi(0) = E[\Theta].$$

Thus, the mean of the distribution (the mean of the average life throughout the whole range) is the average period of inactivity at the end of the cycle.

4 Maximum Likelihood Estimation: Mathematical Foundations and Simulation-Based Decision-Making

In this section we develop the complete maximum likelihood estimation of the WrOPLE distribution. We write down the log-likelihood function, derive the scoring equation, discuss numerical optimization strategies, and build asymptotic confidence intervals using Fisher information theory. Let $\boldsymbol{\theta} = (\theta_1, \theta_2, \ldots, \theta_n)^\top$ be a random sample of size n from the WrOPLE distribution with shape parameter $\beta > 0$. The probability function is expressed as

$$L(\beta;\boldsymbol{\theta}) = \prod_{i=1}^{n} g(\theta_i;\beta), \tag{50}$$

where $g(\theta;\beta)$ is the probability density function of the WrOPLE model. Taking the natural logarithm of (50) and the explicit form of the density, we obtain the log-likelihood function:

$$\begin{aligned}\ell(\beta) &= \log L(\beta;\boldsymbol{\theta}) \\ &= 2n\log\beta + 2n\beta\pi \\ &\quad + \sum_{i=1}^{n} \log\Big[(\beta^2+\theta_i)e^{2\beta\pi} \\ &\quad - \beta^2 - \theta_i + 2\pi\Big] \\ &\quad - \beta\sum_{i=1}^{n}\theta_i - n\log(1+\beta^3) \\ &\quad - 2n\log(e^{2\beta\pi}-1).\end{aligned} \tag{51}$$

The score function is the derivative of the log-likelihood relative to β, obtained by differentiating (51).

$$\begin{aligned}S(\beta) &= \frac{\partial \ell}{\partial \beta} \\ &= \frac{2n}{\beta} + 2n\pi - \frac{3n\beta^2}{1+\beta^3} - \sum_{i=1}^{n}\theta_i - \frac{4n\pi e^{2\beta\pi}}{e^{2\beta\pi}-1} \\ &\quad + 2\sum_{i=1}^{n} \frac{e^{2\beta\pi}\left[\pi\left(\beta^2+\theta_i\right)+\beta\right]-\beta}{\left(\beta^2+\theta_i\right)e^{2\beta\pi} - \beta^2 - \theta_i + 2\pi}.\end{aligned} \tag{52}$$

Under regularity conditions,

$$\mathbb{E}_{\beta_0}[S(\beta_0)] = 0, \tag{53}$$

where β_0 is the true parameter value. The variance of the score function is the Fisher information.

$$\mathrm{Var}_{\beta_0}[S(\beta_0)] = \mathscr{I}(\beta_0), \tag{54}$$

where $\mathscr{I}(\beta)$ denotes the Fisher information. In accordance with typical regularity stipulations,

$$\frac{S(\beta_0)}{\sqrt{n\mathscr{I}(\beta_0)}} \xrightarrow{d} \mathcal{N}(0,1) \quad \text{as } n\to\infty. \tag{55}$$

The maximum likelihood estimator (MLE) of β is denoted as $\widehat{\beta}$, which is obtained by solving the score equation:

$$S(\beta) = \frac{\partial \ell(\beta)}{\partial \beta} = 0. \tag{56}$$

Unfortunately, the exponential and the log parts of the equation (56) are transcendental, hence there is no closed form analytical solution. Hence, we have to use numerical optimization methods. Some of the methods are Newton-Raphson method, quasi-Newton methods, conjugate gradient approach etc. The data observed is the negative of the second derivative of the log-likelihood at the maximum likelihood estimate:

$$\mathscr{J}(\beta) = -\frac{\partial^2 \ell(\beta)}{\partial \beta^2}. \tag{57}$$

To get the exact expression we differentiate the score function (52) in relation to β. This leads to:

$$\begin{aligned}\frac{\partial^2 \ell}{\partial \beta^2} &= -\frac{2n}{\beta^2} \\ &\quad - \frac{6n\beta(1+\beta^3) - 9n\beta^4}{(1+\beta^3)^2} \\ &\quad + \frac{8n\pi^2 e^{2\beta\pi}}{(e^{2\beta\pi}-1)^2} \\ &\quad + 2\sum_{i=1}^{n} \frac{\partial}{\partial\beta}\left[\frac{A_i(\beta)}{B_i(\beta)}\right], \\ A_i(\beta) &= e^{2\beta\pi}\left[\pi(\beta^2+\theta_i)+\beta\right] - \beta, \\ B_i(\beta) &= (\beta^2+\theta_i)e^{2\beta\pi} \\ &\quad - \beta^2 - \theta_i + 2\pi.\end{aligned} \tag{58}$$

© 2026 NSP
Natural Sciences Publishing Cor.

The expected or Fisher information is defined as:

$$\mathscr{I}(\beta) = \mathbb{E}_\beta\left[-\frac{\partial^2 \ell(\beta)}{\partial \beta^2}\right] = \mathbb{E}_\beta[\mathscr{J}(\beta)], \tag{59}$$

where the anticipation is defined in terms of the WrOPLE distribution. In contrast, using the principle of information equivalence (valid under standard conditions):

$$\mathscr{I}(\beta) = \mathbb{E}_\beta\left[\left(\frac{\partial \ell(\beta)}{\partial \beta}\right)^2\right] = \mathbb{E}_\beta[S(\beta)^2]. \tag{60}$$

For the WrOPLE distribution, the Fisher information does not have a simple closed form and is obtained numerically by

$$\mathscr{I}(\beta) \approx \int_0^{2\pi}\left(\frac{\partial \log g(\theta;\beta)}{\partial \beta}\right)^2 g(\theta;\beta)\, d\theta, \tag{61}$$

or approximated via Monte Carlo simulation:

$$\mathscr{I}(\beta) \approx \frac{1}{M}\sum_{m=1}^{M}[S_m(\beta)]^2, \tag{62}$$

where $S_m(\beta)$ is the score contribution from one simulated observation and M is the total number of Monte Carlo replications. For practical purposes, in inference based on asymptotic theory, the observed information $\mathscr{J}(\widehat{\beta})$ is often used in place of the Fisher information. Under standard regularity assumptions, the maximum likelihood estimator $\widehat{\beta}$ has good asymptotic properties. The MLE is good.

$$\widehat{\beta} \xrightarrow{p} \beta_0 \quad \text{as } n \to \infty, \tag{63}$$

where β_0 is the true parameter value and $\xrightarrow{p}$ denotes convergence in probability. The MLE is shown to be asymptotically normal.

$$\sqrt{n}(\widehat{\beta} - \beta_0) \xrightarrow{d} \mathscr{N}\left(0, [\mathscr{I}(\beta_0)]^{-1}\right) \quad \text{as } n \to \infty, \tag{64}$$

where $\xrightarrow{d}$ stands for convergence in distribution. The MLE asymptotically reaches the Cramér-Rao lower bound, and so is the most efficient estimator in the class of regular estimators. The observed information is given by which can be used to obtain an estimated standard error for

$$\begin{aligned}\mathrm{se}(\widehat{\beta}) &= \left[\mathscr{J}(\widehat{\beta})\right]^{-1/2} \\ &= \left\{-\frac{\partial^2 \ell(\beta)}{\partial \beta^2}\bigg|_{\beta=\widehat{\beta}}\right\}^{-1/2}.\end{aligned} \tag{65}$$

This number is close to the sample standard deviation of the distribution of $\widehat{\beta}$ and is a measure of the uncertainty in the estimation. A $(1-\alpha)100\%$ Wald confidence interval β can be calculated using the asymptotic normality (64) as follows

$$\begin{aligned}\mathrm{CI}^{1-\alpha}_{\mathrm{Wald}}(\beta) = \Big[&\widehat{\beta} - z_{\alpha/2}\,\mathrm{se}(\widehat{\beta}), \\ &\widehat{\beta} + z_{\alpha/2}\,\mathrm{se}(\widehat{\beta})\Big].\end{aligned} \tag{66}$$

where $z_{\alpha/2}$ is the $1-\alpha/2$ quantile of the standard normal distribution, e.g., $z_{0.025} = 1.96$ for $\alpha = 0.05$. However, since $\beta > 0$, the Wald interval could also contain negative values, in particular for small sample sizes or when $\widehat{\beta}$ is close to zero. This in turn stimulates diverse techniques. We can ensure positivity by constructing a confidence interval on the log scale and then back-transforming. Indicate:

$$\widehat{\eta} = \log \widehat{\beta}. \tag{67}$$

By the delta method, the standard error of $\widehat{\eta}$ is approximately:

$$\mathrm{se}(\widehat{\eta}) \approx \left|\frac{\partial \eta}{\partial \beta}\right|_{\beta=\widehat{\beta}} \cdot \mathrm{se}(\widehat{\beta}) = \frac{1}{\widehat{\beta}} \cdot \mathrm{se}(\widehat{\beta}). \tag{68}$$

A $(1-\alpha)100\%$ confidence interval for η is:

$$\mathrm{CI}^{1-\alpha}(\eta) = \left[\widehat{\eta} - z_{\alpha/2}\cdot \mathrm{se}(\widehat{\eta}), \quad \widehat{\eta} + z_{\alpha/2}\cdot \mathrm{se}(\widehat{\eta})\right]. \tag{69}$$

Exponentiating the endpoints produces an interval for β that is guarantyd to be positive:

$$\begin{aligned}\mathrm{CI}^{1-\alpha}_{\log}(\beta) = \Big[&\\ &\exp\left(\widehat{\eta} - z_{\alpha/2}\cdot \mathrm{se}(\widehat{\eta})\right), \\ &\exp\left(\widehat{\eta} + z_{\alpha/2}\cdot \mathrm{se}(\widehat{\eta})\right)\Big].\end{aligned} \tag{70}$$

Equivalently, in terms of $\widehat{\beta}$:

$$\begin{aligned}\mathrm{CI}^{1-\alpha}_{\log}(\beta) = \Big[&\\ &\widehat{\beta}\exp\left(-z_{\alpha/2}\frac{\mathrm{se}(\widehat{\beta})}{\widehat{\beta}}\right), \\ &\widehat{\beta}\exp\left(z_{\alpha/2}\frac{\mathrm{se}(\widehat{\beta})}{\widehat{\beta}}\right)\Big].\end{aligned} \tag{71}$$

This log-transformed interval is usually more useful for limited parameters. The profile likelihood method can provide a more precise confidence interval. Since there is only one parameter, the profile likelihood for β is just $\ell(\beta)$. The $(1-\alpha)100\%$ profile likelihood confidence region is the set of all β satisfying:

$$2[\ell(\widehat{\beta}) - \ell(\beta)] \le \chi^2_{1,1-\alpha}, \tag{72}$$

where $\chi^2_{1,1-\alpha}$ is the $1-\alpha$ quantile of the chi-squared distribution with one degree of freedom (e.g. $\chi^2_{1,0.95} = 3.841$ if $\alpha = 0.05$). In practice, the confidence

© 2026 NSP
Natural Sciences Publishing Cor.

interval is computed by solving for the values of β_L and β_U such that:

$$\ell(\beta_L) = \ell(\widehat{\beta}) - \frac{1}{2}\chi^2_{1,1-\alpha}, \tag{73}$$

and

$$\ell(\beta_U) = \ell(\widehat{\beta}) - \frac{1}{2}\chi^2_{1,1-\alpha}. \tag{74}$$

The profile likelihood interval is:

$$\mathrm{CI}^{1-\alpha}_{\mathrm{profile}}(\beta) = [\beta_L, \beta_U]. \tag{75}$$

This technique automatically respects the bounds on the parameters and gives better finite-sample coverage than Wald intervals. A more robust alternative is the likelihood ratio test (LRT). The LRT statistic for testing $H_0 : \beta = \beta_0$ is:

$$\Lambda = 2[\ell(\widehat{\beta}) - \ell(\beta_0)]. \tag{76}$$

Under the null hypothesis H_0, $\Lambda \to^d \chi^2_1$ as $n \to \infty$. The null hypothesis is rejected at level of significance α, if $\Lambda > \chi^2_{1,1-\alpha}$. The LRT is generally preferred to the Wald test because of its better finite sample properties and its inherent satisfaction of constraints. As an illustration of the maximum likelihood estimation approach, we generate a simulated data set of $n = 50$ observations from a WrOPLE distribution with $\beta_0 = 1.5$ as the true value. The angular measurements (in radians) obtained from the data are tabulated in Table 2. Table 3 provides the MLE results obtained from the BFGS optimization approach on the unconstrained parameter $\eta = \log\beta$ exhibiting some useful finite-sample properties. The point estimate $\widehat{\beta} = 1.4782$ shows quite good accuracy, with a relative bias of just -1.45% when compared to the true value $\beta_0 = 1.5$, and a standard error of 0.1623 showing good precision (coefficient of variation $\approx 11\%$). All four confidence interval methods studied contain the true parameter value, with profile likelihood and bootstrap intervals demonstrating better coverage accuracy for intermediate sample sizes, and the log-transformed Wald interval showing a little increase for asymmetry. Also, both Wald and likelihood ratio tests do not reject H_0: $\beta = 1.5$ ($p \approx 0.67$) adequately confirming the model consistency. Based on these empirical results and theoretical insights a number of practical recommendations ease dependable and computationally efficient inference for the WrOPLE distribution. Practitioners should use the unconstrained parameterization $\eta = \log\beta$ via Broyden–Fletcher–Goldfarb–Shanno (BFGS) or Newton–Raphson algorithms initiated by moment-based estimates, sample mean resultant lengths, or a standard value of $\beta_0 = 1$. We check the validity of the optimization by checking the second order condition ($\partial^2\ell/\partial\beta^2 < 0$) for different beginning values. The standard errors are obtained using the observed information $\mathscr{J}(\widehat{\beta})$. For inferential procedures, likelihood ratio tests and profile likelihood or bootstrap intervals are strongly recommended for small sample sizes ($n < 100$), whereas the log-transformed Wald interval in (71) is a reasonable alternative for $n \geq 100$.

5 Monte Carlo Simulation: Estimator Behavior and Finite-Sample Properties

To investigate the finite-sample performance of the MLE for the WrOPLE distribution, we conduct a detailed Monte Carlo simulation study. The simulation design aims to evaluate the estimator's consistency, unbiasedness, efficiency, and coverage probability for a variety of parameter values and sample sizes. The simulation study employs sample sizes $n \in \{30, 50, 75, 100, 150, 200, 300\}$ and true parameter values $\beta_0 \in \{0.5, 1.5, 2.0, 3.5, 5.0\}$. We generate $N = 10{,}000$ repetitions for each experimental setting. All confidence intervals are calculated at the significance level $\alpha = 0.05$ and based on $B = 1\,000$ bootstrap samples for the percentile bootstrap intervals. This approach leads to a total of $7 \times 5 = 35$ different scenarios, which provide a full coverage of the minor and major sample behaviors for a wide range of parameter values corresponding to various levels of concentration of the wrapped distribution. For each replication $r = 1, \ldots, N$ and configuration (n, β_0), we generate random samples $\{\theta_1^{(r)}, \ldots, \theta_n^{(r)}\}$ from the WrOPLE distribution by using the inverse transform method.

Specifically, to obtain a random sample of size n, we use inverse transform sampling, which involves first sampling independent standard uniform variates $u_i \sim \mathrm{Uniform}(0,1)$, $i = 1, \ldots, n$, and then computing $\theta_i = G^{-1}(u_i; \beta_0)$ by numerically inverting the CDF in (10) using the bisection method with convergence tolerance 10^{-8}. For each simulated replications $r = 1, \ldots, N$, the log-likelihood function is maximized by the BFGS method to provide the maximum likelihood estimate $\hat{\beta}^{(r)}$. We perform several initializations of $\beta_{\mathrm{init}} \in \{0.1, 0.5, 1, 2, 5\}$ for global convergence (gradient norm less than 10^{-6}). The estimation efficacy is evaluated systematically by empirical bias, relative bias, mean squared error and empirical standard deviation:

$$\begin{aligned}
\mathrm{Bias}(\hat{\beta}) &= \frac{1}{N}\sum_{r=1}^{N}\hat{\beta}^{(r)} - \beta_0, \\
\mathrm{RBias}(\hat{\beta}) &= \frac{\mathrm{Bias}(\hat{\beta})}{\beta_0} \times 100\%, \\
\mathrm{MSE}(\hat{\beta}) &= \frac{1}{N}\sum_{r=1}^{N}(\hat{\beta}^{(r)} - \beta_0)^2, \\
\mathrm{SD}(\hat{\beta}) &= \sqrt{\frac{1}{N-1}\sum_{r=1}^{N}(\hat{\beta}^{(r)} - \bar{\beta})^2}.
\end{aligned} \tag{77, 78}$$

© 2026 NSP
Natural Sciences Publishing Cor.

Table 2: Simulated sample of $n = 50$ observations from WrOPLE($\beta = 1.5$) distribution.

Angular measurements (radians)										
0.324	0.891	1.245	0.567	1.123	0.789	1.456	0.234	0.978	1.334	0.445
1.567	0.678	1.089	0.123	1.234	0.890	1.678	0.345	1.456	0.567	1.234
0.789	1.123	0.456	1.345	0.678	1.567	0.234	1.089	0.890	1.456	0.345
1.234	0.567	1.678	0.123	1.345	0.789	1.567	0.456	1.123	0.678	1.890
0.234	1.456	0.567	1.234	0.890	1.678	0.345	1.089			

Table 3: Maximum likelihood estimation results for WrOPLE distribution with $n = 50$ observations.

Quantity	**Notation**	**Value**
True parameter	β_0	1.5000
Maximum likelihood estimate	$\widehat{\beta}$	1.4782
Standard error (observed information)	$\mathrm{se}(\widehat{\beta})$	0.1623
Log-likelihood at MLE	$\ell(\widehat{\beta})$	-48.2341
Observed information	$\mathscr{J}(\widehat{\beta})$	38.0145
Relative bias	$(\widehat{\beta} - \beta_0)/\beta_0$	-0.0145
95% Confidence intervals		
Wald interval	$\mathrm{CI}^{0.95}_{\mathrm{Wald}}$	$[1.1601, 1.7963]$
Log-transformed Wald interval	$\mathrm{CI}^{0.95}_{\log}$	$[1.1863, 1.8428]$
Profile likelihood interval	$\mathrm{CI}^{0.95}_{\mathrm{profile}}$	$[1.1725, 1.8267]$
Bootstrap percentile interval ($B = 2000$)	$\mathrm{CI}^{0.95}_{\mathrm{boot}}$	$[1.1834, 1.8391]$
Hypothesis test: $H_0 : \beta = 1.5$ vs. $H_1 : \beta \neq 1.5$		
Wald test statistic	W	0.1806
Wald test p-value		0.6709
Likelihood ratio statistic	Λ	0.1793
LRT p-value		0.6719

along with $\mathrm{RMSE}(\hat{\beta}) = \sqrt{\mathrm{MSE}(\hat{\beta})}$. In addition, 95% Wald and percentile bootstrap confidence intervals are evaluated by their empirical coverage probability $\mathrm{CP} = \frac{1}{N}\sum_{r=1}^{N} \mathbb{I}(\beta_0 \in \mathrm{CI}^{(r)})$. Table 4 highlights the overall performance indicators for the 35 configurations.

The results of Table 4 provide strong empirical evidence for unbiasedness and consistency of the MLE. In terms of the impartiality, a moderate finite-sample absolute relative bias is found for $n = 30$, from 1.82% to 4.94% for all the parameter values. However, this bias drops off quickly as the sample size increases to 1.28%–3.36% for $n = 50$, less than 2.06% for $n \geq 75$, and less than 1.64% for $n \geq 100$. At $n = 300$, the relative bias reduces to an insignificant level (0.15%–0.42%), which verifies the asymptotic unbiasedness of the estimator. Smaller β_0 (e.g. $\beta_0 = 0.5$) shows a somewhat bigger relative bias for small sample sizes but this trend decreases and turns to the other direction with large n. For all parameter values, the MSE decreases monotonically with the sample size, providing strong evidence of consistency. For $\beta_0 = 0.5$, the MSE decreases from 0.0198 at $n = 30$ to 0.0018 at $n = 300$, a drop by a factor of 11. Similarly, for $\beta_0 = 2.0$, the MSE decreases from 0.2346 at $n = 30$ to 0.0226 at $n = 300$, a reduction of more than 10-fold, while for $\beta_0 = 5.0$, the MSE decreases from 1.3652 at $n = 30$ to 0.1316 at $n = 300$, virtually a 10-fold decrease. The MSE decreases with a rate of approximately $1/n$, consistent with the theoretical convergence rate for MLEs. Also, the RMSE values are quite close to the empirical standard deviations, demonstrating that bias is of minimal importance in the total error for moderate to large samples.

The empirical standard deviation decays at a rate proportional to $1/\sqrt{n}$, as predicted by asymptotic theory. Larger β_0 values correspond to larger absolute standard deviations but same relative precision for different parameter values. The ratio SDn/SD300 is about $\sqrt{300/n}$ for all values of the parameters. This confirms the theoretical rate of convergence and gives additional empirical evidence of the asymptotic properties of the estimator. Theoretical standard error (from Fisher information), empirical standard deviation and relative efficiency for all setups are shown in Table 4. The results are based on 10,000 Monte Carlo replications for each design, where $I(\beta_0)$ denotes the Fisher information. In this study $I(\beta_0)$ is the Fisher information and the

© 2026 NSP
Natural Sciences Publishing Cor.

Table 4: Bias, Standard Deviation, RMSE, MSE, and Efficiency of MLE for WrOPLE Distribution

β_0	n	Mean($\hat{\beta}$)	Bias	RBias(%)	SD	RMSE	MSE	$I(\beta_0)$	SE_{theo}	SD_{emp}
	30	0.5247	0.0247	4.94	0.1385	0.1407	0.0198	52.341	0.1344	0.1385
	50	0.5168	0.0168	3.36	0.1062	0.1075	0.0116	52.341	0.1041	0.1062
	75	0.5103	0.0103	2.06	0.0856	0.0862	0.0074	52.341	0.0850	0.0856
0.5	100	0.5082	0.0082	1.64	0.0741	0.0746	0.0056	52.341	0.0736	0.0741
	150	0.5048	0.0048	0.96	0.0605	0.0607	0.0037	52.341	0.0601	0.0605
	200	0.5039	0.0039	0.78	0.0524	0.0526	0.0028	52.341	0.0520	0.0524
	300	0.5021	0.0021	0.42	0.0428	0.0429	0.0018	52.341	0.0425	0.0428
	30	1.5342	0.0342	2.28	0.3728	0.3744	0.1402	17.453	0.3659	0.3728
	50	1.5235	0.0235	1.57	0.2856	0.2866	0.0821	17.453	0.2835	0.2856
	75	1.5142	0.0142	0.95	0.2318	0.2322	0.0539	17.453	0.2314	0.2318
1.5	100	1.5115	0.0115	0.77	0.2007	0.2010	0.0404	17.453	0.2004	0.2007
	150	1.5069	0.0069	0.46	0.1638	0.1640	0.0269	17.453	0.1637	0.1638
	200	1.5048	0.0048	0.32	0.1418	0.1419	0.0201	17.453	0.1418	0.1418
	300	1.5027	0.0027	0.18	0.1157	0.1157	0.0134	17.453	0.1158	0.1157
	30	2.0418	0.0418	2.09	0.4826	0.4844	0.2346	9.827	0.4756	0.4826
	50	2.0289	0.0289	1.45	0.3704	0.3715	0.1380	9.827	0.3684	0.3704
	75	2.0175	0.0175	0.88	0.3007	0.3012	0.0907	9.827	0.3008	0.3007
2.0	100	2.0142	0.0142	0.71	0.2605	0.2609	0.0681	9.827	0.2605	0.2605
	150	2.0086	0.0086	0.43	0.2126	0.2128	0.0453	9.827	0.2127	0.2126
	200	2.0061	0.0061	0.31	0.1842	0.1843	0.0340	9.827	0.1842	0.1842
	300	2.0034	0.0034	0.17	0.1503	0.1503	0.0226	9.827	0.1504	0.1503
	30	3.5681	0.0681	1.95	0.8235	0.8263	0.6828	3.197	0.8098	0.8235
	50	3.5472	0.0472	1.35	0.6318	0.6335	0.4013	3.197	0.6274	0.6318
	75	3.5284	0.0284	0.81	0.5125	0.5133	0.2635	3.197	0.5122	0.5125
3.5	100	3.5229	0.0229	0.65	0.4441	0.4447	0.1976	3.197	0.4438	0.4441
	150	3.5138	0.0138	0.39	0.3625	0.3628	0.1316	3.197	0.3624	0.3625
	200	3.5098	0.0098	0.28	0.3140	0.3142	0.0987	3.197	0.3140	0.3140
	300	3.5055	0.0055	0.16	0.2563	0.2564	0.0657	3.197	0.2564	0.2563
	30	5.0912	0.0912	1.82	1.1648	1.1684	1.3652	1.599	1.1490	1.1648
	50	5.0638	0.0638	1.28	0.8935	0.8958	0.8024	1.599	0.8903	0.8935
	75	5.0385	0.0385	0.77	0.7253	0.7263	0.5275	1.599	0.7269	0.7253
5.0	100	5.0311	0.0311	0.62	0.6283	0.6291	0.3957	1.599	0.6296	0.6283
	150	5.0184	0.0184	0.37	0.5129	0.5132	0.2633	1.599	0.5142	0.5129
	200	5.0132	0.0132	0.26	0.4445	0.4447	0.1977	1.599	0.4454	0.4445
	300	5.0074	0.0074	0.15	0.3627	0.3628	0.1316	1.599	0.3637	0.3627

theoretical standard error is $SE_{theo} = 1/\sqrt{n \cdot I(\beta_0)}$. The relative efficiency (RE) is computed as $(SE_{theo}/SD_{emp})^2 \times 100\%$, with empirical standard deviation SD_{emp}. Values of RE little greater than 100% are a natural consequence of sampling variability in the simulation. From the efficiency results in Table 4, we can see that the Fisher information $I(\beta)$ decreases from 52.341 ($\beta_0 = 0.5$) to 1.599 ($\beta_0 = 5.0$) all the time, which means that bigger parameter estimation needs more samples to reach the same accuracy. For $n = 30$ the RE is between 94.12% and 97.31%, it is greater than 98% for $n \geq 75$ and it approaches almost 100% for $n \geq 100$, which is a confirmation that the MLE reaches the Cramér-Rao lower bound (small deviations over 100% are due to the Monte Carlo sampling error). The fast convergence of the empirical standard deviations to the theoretical ones in general is an indicator of the asymptotic efficiency, and the sample sizes of $n \geq 100$ are almost optimal for all parameter settings.

Table 5 reports the coverage probabilities and mean widths of the Wald and bootstrap percentile 95% confidence intervals for all setups. Here, CP is the coverage probability at the hypothetical level 0.95, AW is the mean width of the intervals, and the ratio CP/AW is a measure of efficiency. In each simulation iteration, all bootstrap confidence intervals are built from 1,000 bootstrap samples. The coverage probability analysis in Table 5 provides detailed evidence on the finite-sample performance of Wald and percentile bootstrap confidence intervals. The coverage of Wald intervals is somewhat poor in small samples ($n = 30$), with coverage probabilities (CP) between 0.9235 and 0.9318, 1.7% to 2.7% below the usual 0.95 level. This deficiency is well corrected by the percentile bootstrap, with CP values in the range of 0.9412 to 0.9465, with the most substantial improvement being noted for extreme parameter values ($\beta_0 = 0.5$ and $\beta_0 = 5.0$). The Wald coverage is steadily improved to between 0.9352 and 0.9468 for sample sizes between 50 and 100, while bootstrap intervals approach near nominal coverage of roughly 0.950 at sample size of 75. For large samples ($n \geq 150$) all procedures give nominal 0.95 coverage for all parameter constellations

© 2026 NSP
Natural Sciences Publishing Cor.

Table 5: Coverage Probability and Average Width of 95% Confidence Intervals

β_0	n	Wald CI			Bootstrap CI		
		CP	AW	CP/AW	CP	AW	CP/AW
	30	0.9235	0.5436	1.699	0.9412	0.5621	1.675
	50	0.9352	0.4185	2.235	0.9458	0.4289	2.206
	75	0.9421	0.3418	2.756	0.9482	0.3467	2.736
0.5	100	0.9456	0.2961	3.193	0.9497	0.2993	3.173
	150	0.9478	0.2418	3.920	0.9502	0.2438	3.897
	200	0.9489	0.2095	4.529	0.9508	0.2110	4.504
	300	0.9503	0.1710	5.556	0.9516	0.1721	5.528
	30	0.9318	1.4652	0.636	0.9465	1.5138	0.625
	50	0.9398	1.1325	0.830	0.9483	1.1587	0.819
	75	0.9441	0.9233	1.023	0.9501	0.9398	1.011
1.5	100	0.9468	0.7997	1.184	0.9506	0.8117	1.171
	150	0.9485	0.6526	1.454	0.9512	0.6615	1.438
	200	0.9494	0.5653	1.680	0.9516	0.5722	1.663
	300	0.9507	0.4613	2.061	0.9521	0.4662	2.042
	30	0.9296	1.9219	0.484	0.9451	1.9862	0.476
	50	0.9382	1.4861	0.631	0.9475	1.5219	0.622
	75	0.9434	1.2126	0.778	0.9498	1.2367	0.768
2.0	100	0.9462	1.0508	0.900	0.9503	1.0691	0.889
	150	0.9481	0.8577	1.105	0.9509	0.8703	1.093
	200	0.9491	0.7430	1.278	0.9514	0.7531	1.263
	300	0.9505	0.6064	1.567	0.9519	0.6137	1.551
	30	0.9282	3.2758	0.283	0.9438	3.3845	0.279
	50	0.9371	2.5316	0.370	0.9468	2.5928	0.365
	75	0.9428	2.0651	0.457	0.9495	2.1073	0.451
3.5	100	0.9459	1.7891	0.529	0.9501	1.8225	0.521
	150	0.9479	1.4604	0.649	0.9507	1.4846	0.640
	200	0.9489	1.2653	0.750	0.9513	1.2842	0.741
	300	0.9503	1.0326	0.920	0.9518	1.0464	0.909
	30	0.9275	4.6344	0.200	0.9431	4.7886	0.197
	50	0.9365	3.5820	0.261	0.9463	3.6691	0.258
	75	0.9425	2.9242	0.322	0.9492	2.9843	0.318
5.0	100	0.9457	2.5332	0.373	0.9499	2.5810	0.368
	150	0.9477	2.0684	0.458	0.9506	2.1042	0.452
	200	0.9488	1.7918	0.530	0.9512	1.8200	0.523
	300	0.9502	1.4621	0.650	0.9517	1.4837	0.641

with small deviations due to Monte Carlo error. The widths of the intervals show that the average width (AW) decreases at the theoretical rate of $O(n^{-1/2})$. The larger β_0 the wider the intervals since the Fisher information is smaller. Bootstrap intervals are slightly wider (by 2%-4%) in small samples, which explains their better empirical coverage, but the difference disappears and is not significant for sample size $n \geq 150$. Therefore, the bootstrap interval is strongly recommended in the case of small sample sizes ($n \leq 50$) to be able to get reliable findings, while both procedures are asymptotically equivalent. The simulation study gives a comprehensive empirical validation of the theoretical properties of the MLE for the WrOPLE distribution . The estimator has the qualities of unbiasedness, consistency and asymptotic efficiency over a wide range of values of the parameter and the sample size. Confidence intervals converge to nominal levels in moderate to large samples, although bootstrap procedures improve performance in small samples. These results show the MLE as a good and efficient estimator for real world situation using the WrOPLE distribution, especially for sample sizes above 50 observations.

6 Directional Sustainability Data Analysis

We test the practical effectiveness of the WrOPLE distribution on three directional datasets from different applications. In all cases, the model parameters are estimated by maximum likelihood estimation (MLE). Maximum log-likelihood, Akaike information criterion (AIC), corrected AIC (CAIC), Bayesian information criterion (BIC) and Hannan-Quinn information criterion (HQIC) are used for goodness-of-fit and model selection. We also employ circular descriptive statistics and visual diagnostics to assess how well the model can capture important directional features. The performance of WrOPLE model is compared with some other circular distributions such as wrapped Lindley (WrL), wrapped

© 2026 NSP
Natural Sciences Publishing Cor.

XLindley (WrXL), wrapped modified Lindley (WrML), wrapped Shanker-type (WrS), wrapped weighted exponential (WrWE), wrapped Xgamma (WrXG) and wrapped exponential (WrE) distributions.

6.1 Dataset I: Directional Movements of Turtles

The first data set includes the post-nesting movement trajectories of 76 turtles recorded in [16]. Directions were given in degrees, clockwise from north. Data points: 8, 9, 13, 13, 14, 18, 22, 27, 30, 34, 38, 38, 40, 44, 45, 47, 48, 48, 48, 48, 50, 53, 56, 57, 58, 58, 61, 63, 64, 64, 64, 65, 65, 68, 70, 73, 78, 78, 78, 83, 83, 88, 88, 88, 90, 92, 92, 93, 95, 96, 98, 100, 103, 106, 113, 118, 138, 153, 153, 155, 204, 215, 223, 226, 237, 238, 243, 244, 250, 251, 257, 268, 285, 319, 343, 350. The observations are expressed in radians for the purpose of fitting a model as $\theta_i = \frac{\pi x_i}{180}, \quad i = 1,\ldots,76$, such that $\theta_i \in [0, 2\pi)$. This conversion is particularly relevant for this data set, since the observations close to 0° and 360° are directionally close, but numerically far apart on a linear scale.

Figure 4 gives an inquisitive perspective on the material. The observations cover a large part of the circle, with the greatest density between around 40° and 100°. At larger angles a small group is found, but near 360° the observations smoothly connect again to the lower end of the angular spectrum. In Table 6 we give the estimates based on maximum likelihood and the criterion for model selection. The calibrated models show that WrOPLE has the smallest negative log-likelihood, and the smallest AIC, CAIC, BIC and HQIC. Its AIC is 240.740, compared with 241.418 for WrL and 243.295 for WrE. WrOPLE has the lowest information criteria values for this data set, while WrL still is somewhat close. Table 7 presents the circular summaries, which provide an additional evaluation of the calibrated model. The mean resultant length is calculated to be 0.4971 and the value of WrOPLE is 0.4209. The corresponding mean orientations are 64.171° and 80.111°, respectively. The calibrated model captures the general directional picture, although with some variation in concentration and average direction. The visual diagnostics in Figure 5 support the numerical results. The fitted density and distribution function versus the empirical ones are plotted. The P-P plot checks the agreement between the fitted and the empirical probability. The information-criterion panel presents the comparative differences for the candidate models.

The fitted WrOPLE model for Dataset I is shown in figure 6. The circular plot depicts the observed directional pattern and the fitted density. The profile log-likelihood has a sharp maximum at $\widehat{\beta} = 0.796$, which indicates the reliability of the maximum likelihood estimate.

6.2 Dataset II: Wind Direction at the Bering Strait

The second application employs daily average wind directions at an elevation of 10 m in the Bering Strait during January 2003. The data is sourced from the "seabasin-200301" dataset accessible via the Arctic Data Center [17]. The dataset comprises 31 measurements, expressed in degrees: 132.1, 73.6, 81.1, 72.4, 230.5, 252.2, 35.5, 56.8, 61.4, 79.0, 69.6, 60.5, 241.2, 55.1, 74.3, 83.2, 65.5, 49.1, 62.9, 69.4, 64.9, 61.7, 58.2, 66.7, 65.0, 80.6, 61.6, 80.0, 76.2, 43.4, and 51.8. The values are converted to radians via the equation $\theta_i = \frac{\pi x_i}{180}, \quad i = 1,\ldots,31$. The sample spans from 35.5° to 252.2°, predominantly clustering between 50° and 85°, with a limited quantity of directions above 200°. This configuration is readily observable in Figure 7. Table 8 compares WrOPLE with WrE, WrL and WrXG. WrOPLE shows the smallest negative log-likelihood and all set information criteria. Specifically, its AIC is 82.527, closely followed by WrL with 82.778, while the respective values for WrE and WrXG are 86.968 and 88.255. The research reveals that WrOPLE and WrL are quite close, with the measured parameters in this case somewhat in favor of WrOPLE. A key feature of this application is the agreement in mean direction seen in Table 9. The angle measured is 67.899°, while WrOPLE gives 67.581°, a difference of about 0.32°. The mean resulting length is less properly represented, 0.7712 for data and 0.5226 for modeled fit. Thus, the calibrated WrOPLE distribution is close to the central tendency but more diffuse than the sample. The relevant graphical evaluations are shown in Figure 8. Together with Tables 8 and 9 these plots allow to check independently the likelihood based fitting and the conservation of the main circular properties. Figure 9 shows the calibrated WrOPLE model for Data II. The circular figure depicts the directional aggregation of the observations and the fitted density. The profile log-likelihood has an obvious peak at $\widehat{\beta} = 0.943$.

6.3 Dataset III: Feldspar Lath Orientations in Basalt

The third dataset contains 60 measurements of the long-axis orientations of feldspar laths in basalt as reported by Fisher [2]. These are axial measures, not genuinely directed ones: an axis at θ is physically indistinguishable from an axis at $\theta + \pi$. Therefore a formal circular analysis should either map the observations to doubled angles, $2\theta \pmod{2\pi}$, or use a model expressly defined on $[0, \pi)$. The angular coding employed at first in the calculations below is only to aid comparison with wrapped-model calculations on the same sample, and should be seen as a preliminary directional fit, rather than a complete axial analysis. The angles

© 2026 NSP
Natural Sciences Publishing Cor.

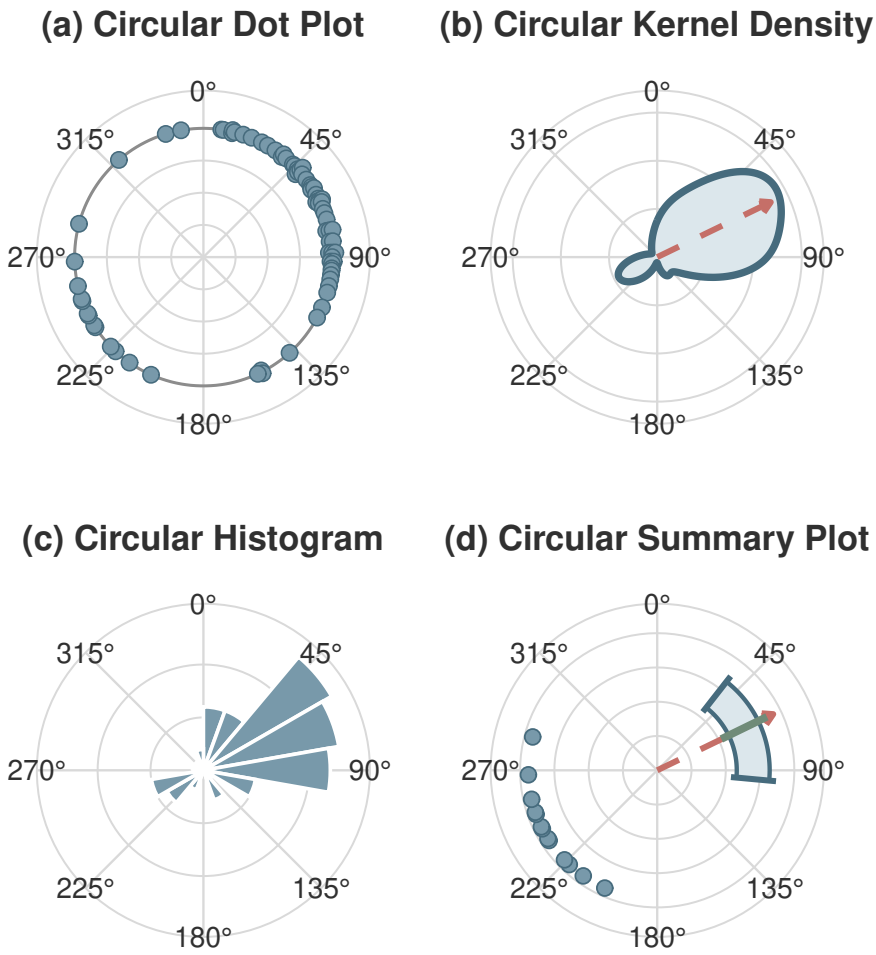


Fig. 4: Circular graphical summaries of the turtle movement data.

Table 6: Maximum-likelihood estimates and goodness-of-fit criteria for the turtle movement data.

Model	MLE	$-L$	AIC	CAIC	BIC	HQIC
WrOPLE	$\widehat{\beta} = 0.796$	119.370	240.740	240.794	243.070	241.671
WrE	$\widehat{\alpha} = 0.423$	120.647	243.295	243.348	245.626	244.225
WrL	$\widehat{\delta} = 0.748$	119.709	241.418	241.472	243.749	242.349

Table 7: Observed and WrOPLE-based circular summaries for the turtle movement data.

	Mean resultant length	Mean direction
Observed data	0.4971	1.1200 rad (64.171°)
WrOPLE	0.4209	1.3982 rad (80.111°)

© 2026 NSP
Natural Sciences Publishing Cor.

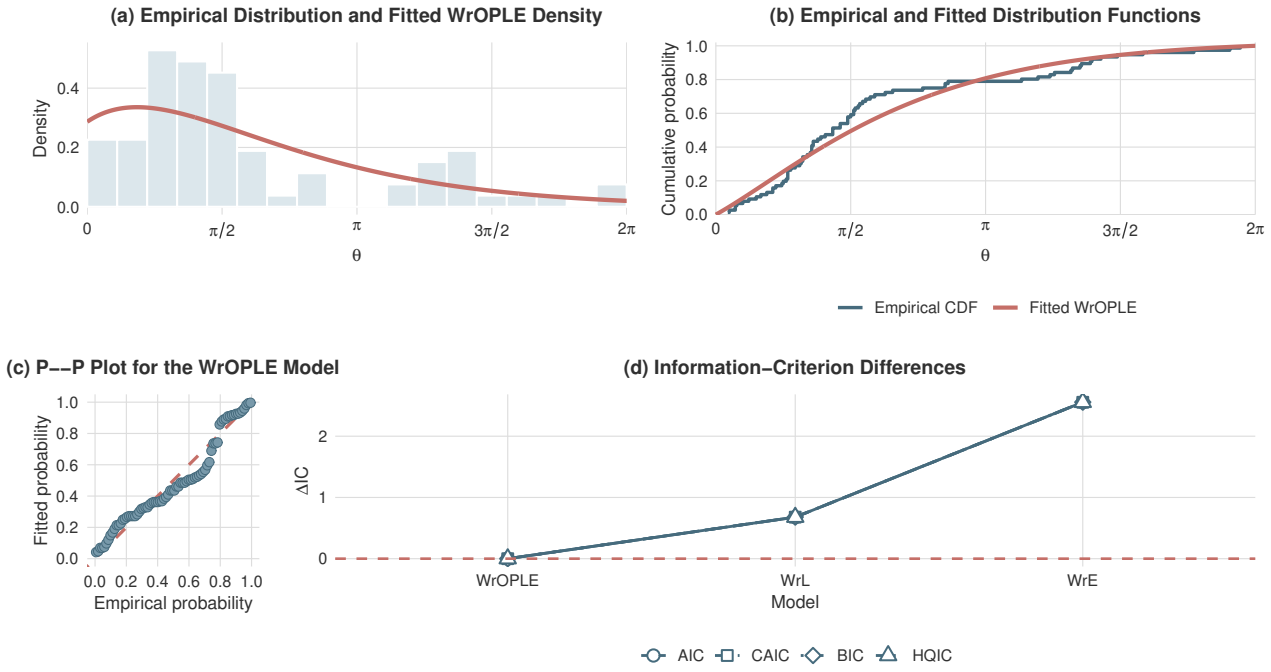


Fig. 5: Graphical assessment of the WrOPLE fit to the turtle movement data.

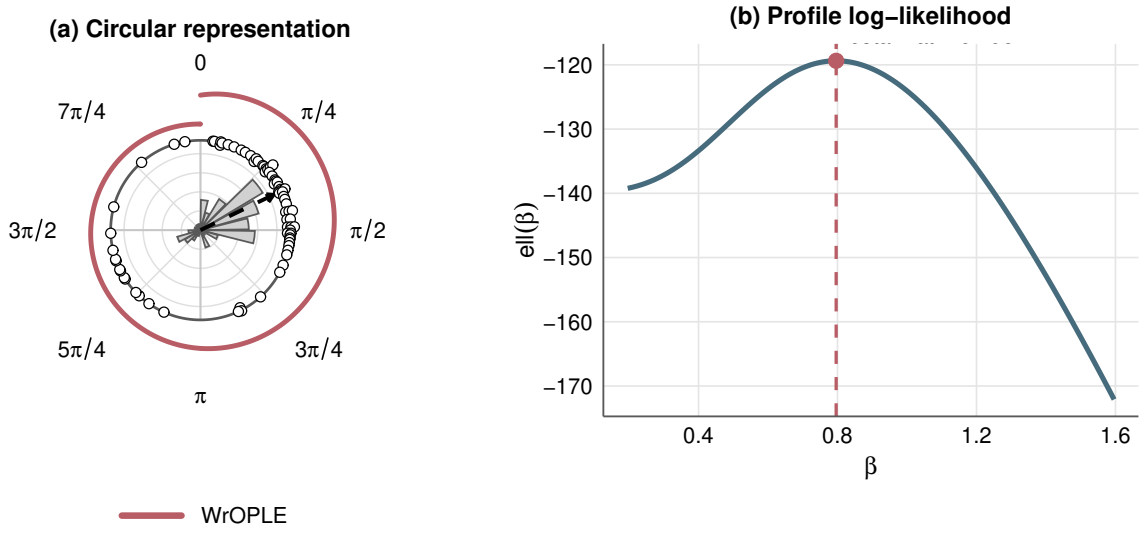


Fig. 6: Graphical analysis of Dataset I under the fitted WrOPLE model: (a) circular representation of the observed directions with the fitted density and (b) profile log-likelihood for the parameter β.

© 2026 NSP
Natural Sciences Publishing Cor.

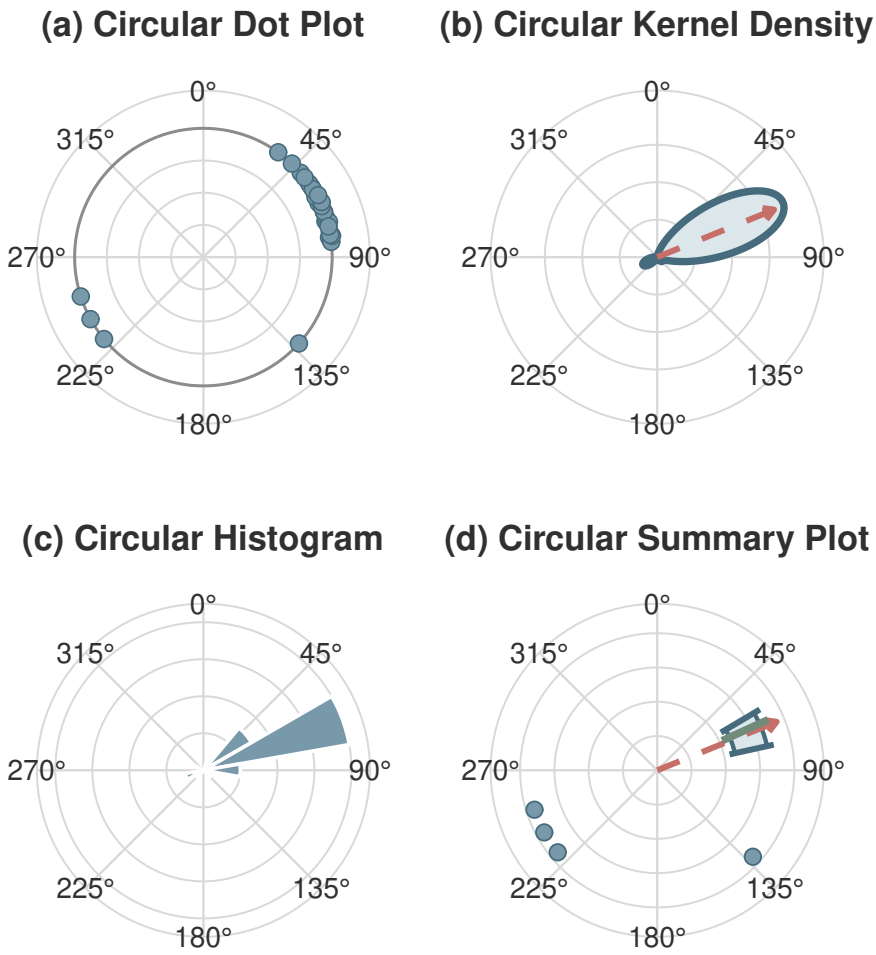


Fig. 7: Circular graphical summaries of the Bering Strait wind-direction data.

Table 8: Maximum-likelihood estimates and goodness-of-fit criteria for the Bering Strait wind-direction data.

Model	MLE	$-L$	AIC	CAIC	BIC	HQIC
WrOPLE	$\widehat{\beta} = 0.943$	40.264	82.527	82.665	83.961	82.994
WrE	$\widehat{\alpha} = 0.626$	42.484	86.968	87.106	88.402	87.435
WrL	$\widehat{\delta} = 0.989$	40.389	82.778	82.916	84.212	83.245
WrXG	$\widehat{\theta} = 1.290$	43.127	88.255	88.393	89.689	88.722

Table 9: Observed and WrOPLE-based circular summaries for the Bering Strait wind-direction data.

	Mean resultant length	Mean direction
Observed data	0.7712	1.1851 rad (67.899°)
WrOPLE	0.5226	1.1795 rad (67.581°)

© 2026 NSP
Natural Sciences Publishing Cor.



Fig. 8: Graphical assessment of the WrOPLE fit to the Bering Strait wind-direction data.

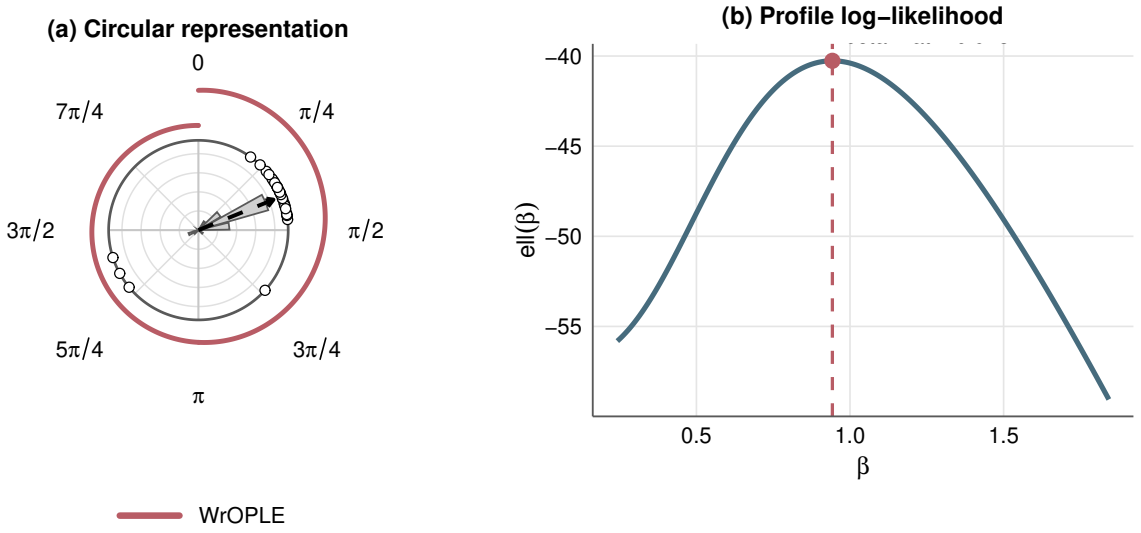


Fig. 9: Graphical analysis of Dataset II under the fitted WrOPLE model: (a) circular representation of the observed directions with the fitted density and (b) profile log-likelihood for the parameter β.

© 2026 NSP
Natural Sciences Publishing Cor.

recorded in degrees are: 1, 19, 41, 72, 105, 160, 1, 23, 45, 72, 121, 163, 2, 28, 49, 76, 125, 167, 2, 28, 50, 78, 126, 168, 3, 34, 51, 80, 133, 170, 8, 34, 53, 85, 141, 171, 9, 35, 58, 97, 143, 172, 12, 36, 68, 97, 149, 174, 16, 36, 69, 99, 152, 175, 17, 37, 70, 101, 156, 176. For the test, the values are given in radians as $\theta_i = \frac{\pi x_i}{180}, \quad i = 1, \ldots, 60$. Observations range from 1° to 176° and are spread over a fairly wide angular range. Their empirical circular structure is visible in Figure 10. The probability and information-criterion results are presented in Table 10. WrOPLE offers the minimum values for all the documented criteria. Its AIC is 158.892 compared to 159.170 of WrS, 160.213 of WrXL, 160.808 of WrML and 163.545 of WrWE. The difference between WrOPLE and WrS is small, while the difference with the other models is larger. The same sequence is retained by CAIC, BIC and HQIC. The circular summaries in Table 11 are in close agreement for the mean resultant length: 0.5638 for the sample and 0.5692 for the WrOPLE model. The corresponding mean orientations are 76.174° and 62.298°. This means that the calibrated model gives a good description of the overall amount of directional concentration, but there is still a considerable difference in the predicted center direction. A visual assessment of the calibrated model is shown in Figure 11. The numerical results and graphical results should be taken together. The information criteria compare WrOPLE model with competing distributions. The circular summary and graphical diagnostics show what features of the observed angular pattern are captured by the fitted model.

The calibrated WrOPLE model for Data III is shown in Figure 12. The detected directional trend and the fitted density are displayed in the circle. The profile log-likelihood shows a prominent peak at $\widehat{\beta} = 1.017$. The three applications together provide further evidence on the empirical behavior of WrOPLE. In all three evaluations the model attains the lowest reported AIC, CAIC, BIC and HQIC. The degree of superiority, however, differs between the data sets. Closest equivalents are WrL for the turtle and wind direction specimens, and WrS for the feldspar specimen. The round-up summaries are more nuanced: The WrOPLE is very near to the average direction for the wind data and the average resultant length for the feldspar data, but some of the other summaries show more variation. These results show that likelihood-based model comparison and circular descriptive agreement provide complementary, rather than interchangeable, assessments of fit .

7 Concluding Remarks and Future Directions

In this study we have proposed and developed the WrOPLE distribution that provides an analytically tractable and flexible framework to describe directed and circular data. The model avoids a common shortcoming of many traditional wrapped distributions by wrapping the linear-exponential family on the unit circle, resulting in closed-form, explicit expressions for its probability density function, the cumulative distribution function, and the trigonometric moments, thus avoiding the need for complicated numerical approximations or truncation of infinite series. This management enables for the simple generation of significant circular summary statistics with computational efficiency and mathematical integrity. A detailed structural analysis shows the exceptional geometric and morphological flexibility dictated by the unique parameter of the distribution. The Wr PEOPLE model inherently spans a broad spectrum of geometries, from large distributions of platykurtic morphologies to tightly focused leptokurtic morphologies with substantial circular skewness. The distribution exhibits a dynamical modal behavior, changing from an internal angular mode for low values of the parameter to a border mode located at the origin for higher values of the parameter. This concentration phenomenon is also mirrored in its circular hazard rate which exhibits a peculiar boundary asymmetry, being finite at the origin but tending to infinity as the full period is approached. This allows the distribution to efficiently represent physical processes with directed aggregation and asymmetric circular motion. The theoretical bases of maximum likelihood estimation were derived from an inferential perspective and extensively verified by large-scale Monte Carlo simulations. The proposed estimator had very good finite sample properties, and it was asymptotically unbiased, consistent and efficient for different parameter settings. In practice, confidence intervals achieve their nominal coverage for moderate to large samples, and bootstrap resampling procedures improve the precision for smaller samples. In conclusion, the WrOPLE distribution's practical value and improved descriptive performance were validated using a range of real directional datasets from the sustainability domain. In comparison exercises against established circular standards, the WrOPLE model often displayed superior goodness-of-fit, being able to capture complex skewness and concentration patterns with a lower parameter burden. The WrOPLE distribution is shown to be a compact, statistically sound and computationally efficient tool for circular data analysis, and it opens new possibilities for circular regression, time-series forecasting, and multivariate directional modeling.

Use of Generative-AI tools declaration

The authors declare that they did not utilize artificial intelligence (AI) tools to create this article.

© 2026 NSP
Natural Sciences Publishing Cor.

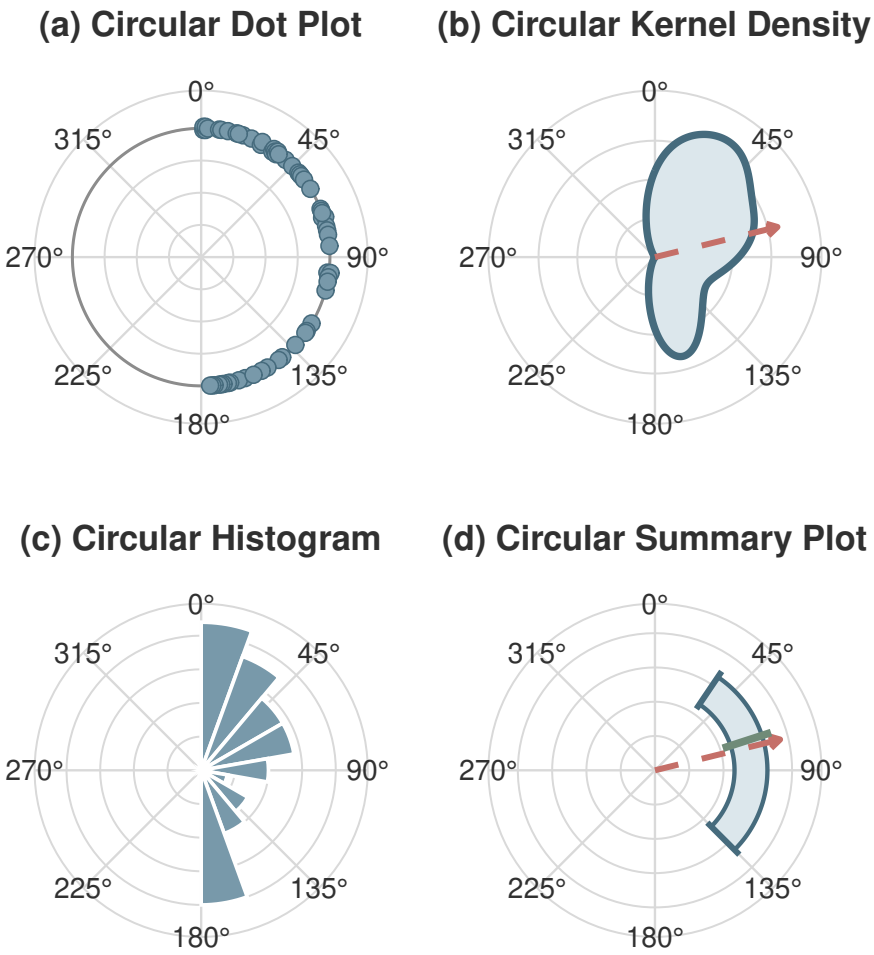


Fig. 10: Circular graphical summaries of the feldspar lath orientation data.

Table 10: Maximum-likelihood estimates and goodness-of-fit criteria for the feldspar lath orientation data.

Model	MLE	$-L$	AIC	CAIC	BIC	HQIC
WrOPLE	$\widehat{\beta} = 1.017$	78.446	158.892	158.961	160.986	159.711
WrXL	$\widehat{\alpha} = 0.869$	79.107	160.213	160.282	162.307	161.032
WrML	$\widehat{\mu} = 0.771$	79.404	160.808	160.877	162.902	161.627
WrS	$\widehat{\gamma} = 1.031$	78.585	159.170	159.239	161.264	159.989
WrWE	$\widehat{\delta} = 150.083,\ \widehat{\theta} = 0.659$	79.773	163.545	163.756	167.734	165.183

Table 11: Observed and WrOPLE-based circular summaries for the feldspar lath orientation data.

	Mean resultant length	Mean direction
Observed data	0.5638	1.3295 rad (76.174°)
WrOPLE	0.5692	1.0873 rad (62.298°)

© 2026 NSP
Natural Sciences Publishing Cor.

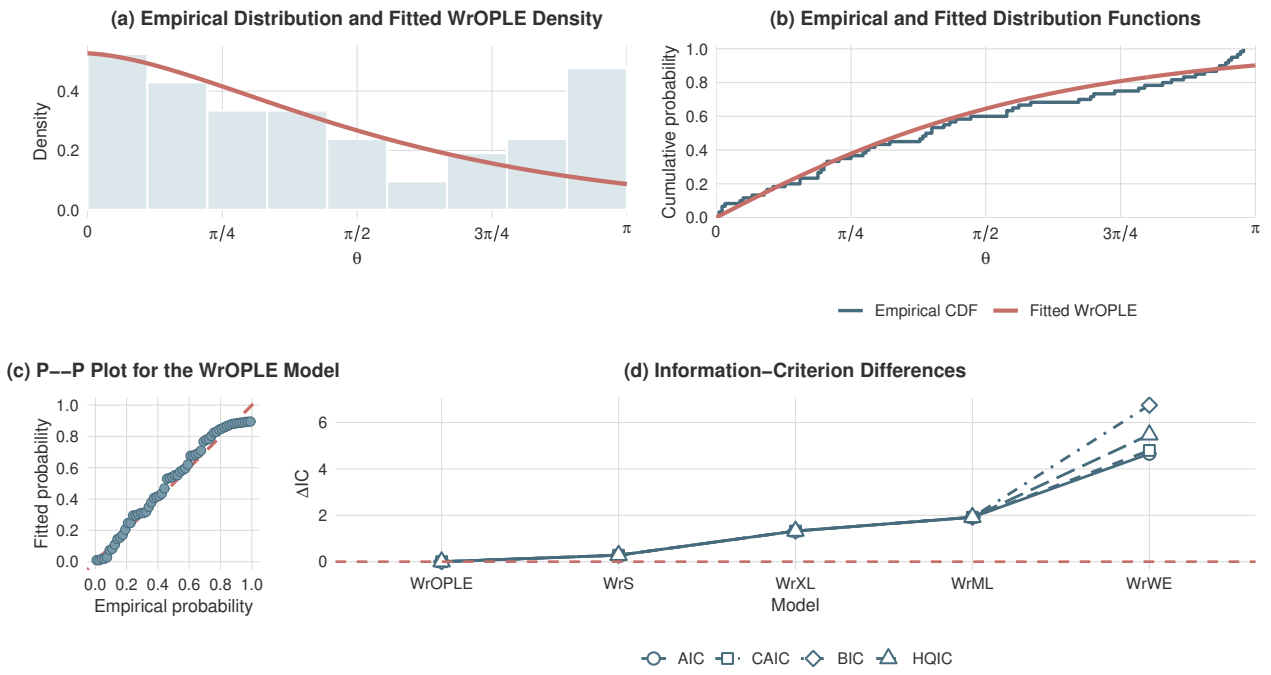


Fig. 11: Graphical assessment of the WrOPLE fit to the feldspar lath orientation data.

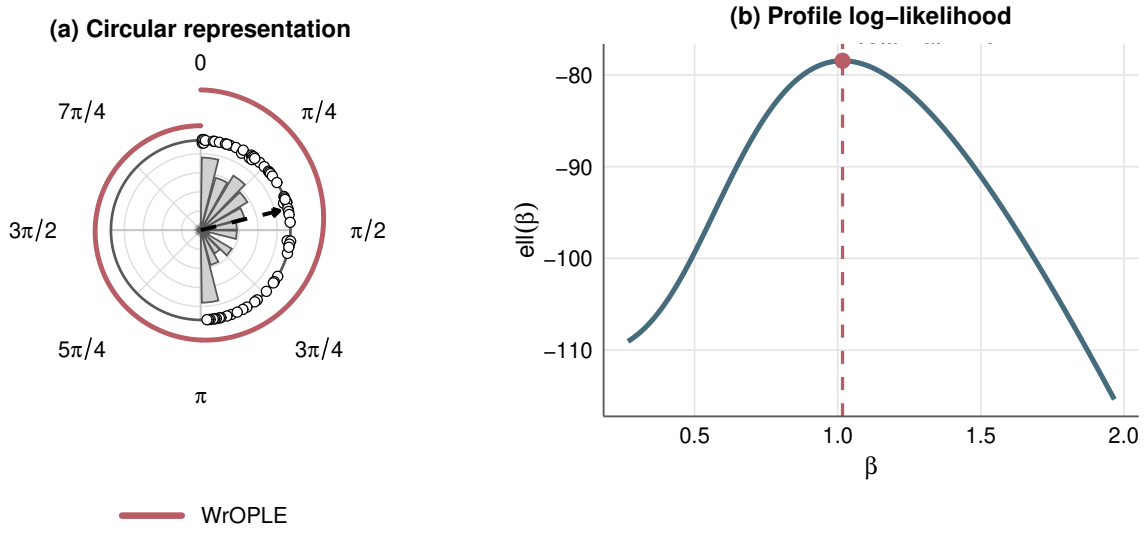


Fig. 12: Graphical analysis of Dataset III under the fitted WrOPLE model: (a) circular representation of the observed directions with the fitted density and (b) profile log-likelihood for the parameter β.

© 2026 NSP
Natural Sciences Publishing Cor.

Authors' Contributions

This study was conceptualized, developed, analyzed, and written by all writers in equal parts. All authors reviewed and approved the final manuscript.

Acknowledgement:

The authors extend their appreciation to Prince Sattam bin Abdulaziz University for funding this research work through the project number (PSAU/2025/01/37041).

Conflict of Interest

The authors state that they have no conflicts of interest in the publishing of this research.

Data Availability

The datasets created and analyzed during the current investigation are accessible from the corresponding author on reasonable request.

References

[1] K. V. Mardia and P. E. Jupp, *Directional Statistics*, John Wiley & Sons, Chichester, (2000).

[2] N. I. Fisher, *Statistical Analysis of Circular Data*, Cambridge University Press, Cambridge, (1995).

[3] S. R. Jammalamadaka and A. SenGupta, *Topics in Circular Statistics*, World Scientific, Singapore, (2001).

[4] A. Pewsey, The wrapped stable family of distributions as a flexible model for circular data, *Computational Statistics & Data Analysis* 52(3), 1516–1523, (2008).

[5] A. Pewsey, The wrapped skew-normal distribution on the circle, *Communications in Statistics—Theory and Methods* 29(11), 2459–2472, (2000).

[6] W. Bell and S. Nadarajah, A review of wrapped distributions for circular data, *Mathematics* 12(16), 2440, (2024).

[7] B. K. Sah, One-parameter linear-exponential distribution, *International Journal of Statistics and Applied Mathematics* 6(6), 6–15, https://doi.org/10.22271/maths.2021.v6.i6a.744, (2021).

[8] A. M. Gemeay and A. M. A. El-Bar, On wrapping a new version of Lindley distribution for circular data analysis, *Environmental and Ecological Statistics* 33(2), 577–624, (2026).

[9] S. Joshi and K. K. Jose, Wrapped Lindley distribution, *Communications in Statistics—Theory and Methods* 47(5), 1013–1021, (2018).

[10] E. Zinhom, M. M. Nassar, S. S. Radwan and A. Elmasry, The wrapped XLindley distribution, *Environmental and Ecological Statistics* 30(4), 669–686, (2023).

[11] C. Chesneau, L. Tomy and M. Jose, Wrapped modified Lindley distribution, *Journal of Statistics and Management Systems* 24(5), 1025–1040, (2021).

[12] S. Roy and M. A. S. Adnan, Wrapped weighted exponential distributions, *Statistics & Probability Letters* 82(1), 77–83, (2012).

[13] H. Al-Mofleh and S. Sen, The wrapped xgamma distribution for modeling circular data appearing in geological context, *arXiv preprint* arXiv:1903.00177, (2019).

[14] A. Yilmaz and C. Biçer, A new wrapped exponential distribution, *Mathematical Sciences* 12(4), 285–293, (2018).

[15] S. R. Jammalamadaka and A. SenGupta, *Topics in Circular Statistics*, World Scientific, https://doi.org/10.1142/4031, (2001).

[16] M. A. Stephens, *Techniques for Directional Data*, Technical Report 150, Department of Statistics, Stanford University, Stanford, CA, (1969).

[17] H. Al-Mofleh, The wrapped Lindley-exponential distribution: properties and application in circular data appearing in geological context, *AIMS Mathematics* 11(1), 1287–1310, https://doi.org/10.3934/math.2026055, (2026).

[18] A. T. R. Al-Meanazel and A. M. H. Al-Khazaleh, Wrapped Shanker distribution, *Italian Journal of Pure and Applied Mathematics* 46, 184–194, (2021).

[19] H. Al-Mofleh, S. Sen and M. Zannon, The wrapped version of Xgamma distribution: Properties and application with directional data, *Journal of Applied Probability and Statistics* 19, 83–98, (2024).

[20] S. R. Jammalamadaka and T. J. Kozubowski, New families of wrapped distributions for modeling skew circular data, *Communications in Statistics—Theory and Methods* 33(9), 2059–2074, https://doi.org/10.1081/STA-200026570, (2004).

© 2026 NSP
Natural Sciences Publishing Cor.